FINAL REPORT

NAG 5-1282

DUST NEAR LUMINOUS ULTRAVIOLET STARS

prepared by

Richard C. Henry

Principal Investigator

Due September 30, 1993

FINAL REPORT on NAG 5-1282

DUST NEAR LUMINOUS ULTRAVIOLET STARS

Richard C. Henry, Principal Investigator

This is the final report on the referenced NASA grant. The major product of the work is of course the published results in the refereed literature, above all in the Astrophysical Journal. I begin, therefore, by presenting a bibliography of papers published by me that are a result of the grant in question, or related grants and contracts where the work is closely related to the work performed under this grant:

109. (with W. B. Landsman, J. Murthy, P. D. Tennyson, J. B. Wofford, and R. Wilson), Atlas of the Ultraviolet Sky, Johns Hopkins University Press, Baltimore (1988).

112. (with H. Walker, M. Werner, C. Allen, R. Kimble, J. Wofford, and J. Murthy), Studying the Spatial Distribution of Interstellar Dust; Interstellar Dust: Contributed Papers, ed. A. G. G. M. Tielens and L. J. Allamandola, NASA Conference Publication 3036, 313 (1988).

119. (with J. Murthy, R. C. Henry, R. A. Kimble, J. B. Wofford, M. W. Werner, and H. G. Walker), Emission from Dust Near High Latitude Stars; The Galactic and Extragalactic Background Radiation, ed. S. Bowyer and C. Leinert, IAU Symposium No. 139, Kluwer Academic Publishers, 237 (1990).

120. (with J. Murthy, H. W. Moos, A. Vidal-Madjar,J. L. Linsky, and C. Gry), Studies of HI and DI in the Local Interstellar Medium, Astrophys. J., **356**, 223 (1990).

123. (with Jayant Murthy, and J. B. Holberg), Constraints on the Optical Properties of Interstellar Dust in the Far Ultraviolet: *Voyager* Observations of the Diffuse Sky Background, Astrophys. J., **383**, 198 (1991).

125. Ultraviolet Background Radiation; Annual Review of Astronomy and Astrophysics, **29**, 89 (1991).

132. (with J. Murthy and H. J. Walker), The Low Filling Factor of Dust in the Galaxy, Astrophys. J., **401**, 574 (1992).

134. (with J. Murthy, A. Dring, J. W. Kruk, W. P. Blair, R. A. Kimble, and S. T. Durrance), Hopkins Ultraviolet Telescope Observations of FUV Scattering in NGC 7023: the Dust Albedo; Astrophys. J., **408**, L97 (1993).

135. (with A. N. Witt, J. K. Petersohn, J. B. Holberg, J. Murthy, and A. Dring), *Voyager 2* Observations of NGC 7023: Dust Scattering Shortward of 1600 Å; Astrophys. J.,**410**, 714 (1993).

137. (with J. Murthy, M. Im, and J. B. Holberg), *Voyager* Observations of Diffuse Far-Ultraviolet Continuum and Line Emission in Eridanus; Astrophys. J., **419**, 739 (1993).

139. (with J. Murthy and J. B. Holberg), *Voyager* Observations of Dust Scattering Near the *Coalsack* Nebula; Astrophys. J., **428**, 233 (1994).

142. (with A. R. Dring, J. Murthy, and H. J. Walker), The Distribution of Dust Clouds in the Interstellar Medium; Astrophys. J. (submitted), (1994).

Of these, the papers that are a specific product of the present grant (or our preceding IRAS activity) are papers # 109, 112, 119, 132, and 142 above. That is, for those papers a credit line to the IRAS grant or contract appears in the publication.

The other papers are directly related in the sense that they are part of my overall effort to understand the nature of the diffuse ultraviolet (not a misprint!) background. Specifically, the reason I proposed on IRAS was to better understand the nature and optical properties of dust at moderate and high galactic latitudes.

The reason that this was of importance is that my fundamental research program is directed toward the elucidation of the nature of the diffuse ultraviolet background. Now at low galactic latitudes, one expects that there will be diffuse ultraviolet scattered starlight, just as there is in the visible. Again, looking toward moderate and high galactic latitudes, one expects at some level to find ultraviolet starlight scattering from dust.

That is where IRAS came in: the "cirrus" discovered using IRAS is thermal radiation from interstellar dust at moderate and high galactic latitudes. Thus, IRAS locates the dust. It is this dust which must (at some level) scatter ultraviolet starlight. However, it was not clear to us whether the cirrus that was observed was the whole thermal radiation from dust, or whether we were simply seeing the "tip of the iceberg" and the structure that is observed was not on top of a more or less uniform distribution of dust that would not be revealed by IRAS because of zero-level determination problems. IRAS, after all, was not created with the idea of studying diffuse radiation; it was intended for point sources. The diffuse radiation was a bonus.

It occurred to me, that it might be possible to distinguish what was going on, by looking for IRAS thermal emission in the direction of bright stars. The idea was (and is) that such stars must heat LOCAL dust near those stars, and if the stars are located in a region of essenially uniform emission that we would not be aware of normally using IRAS (thingking that we were simply seeing instrumental background), the emission from the dust would be revealed.

We have worked hard on this, with mixed results. Certainly we have acquired and published a mass of data on the topic. But it is hard to interpret the results. We had expected to find thermal emission around virtually every star; instead, most stars show no detectable emission. And when we do find emission, it is not uniform emission: it is not that the star is embedded in "an interstellar medium." Instead, we find discrete clouds that are heated by the starlight. The clouds are not associated with the star; it is just chance that the cloud happens to be near the star at this particular time, and is illuminated.

The exception is that we find a dearth of clouds near the very hottest stars, and by a substantial factor. The implication is that the very hottest stars play an active role with respect to the dust clouds, destroying them or modifying them substantially over time. The other possiblility is simply that the hottest stars are located in regions lacking in dust, which is very counterintuitive.

We intend to continue our work with the IRAS data under other auspices, though we do not rule out the thought that we might propose again as an ADP IRAS program. The work that we are currently doing to extend the work done under the present grant, is work that is supported by the US Air Force, where we are preparing an electronic model of the diffuse ultraviolet radiation over the sky. The IRAS data continue to play their basic role (for us) as tracer of dust, which in turn scatters ultraviolet starlight.

To complete this report, I attach a reprint of our paper #132 in the Astrophysical Journal, and a preprint of paper #142 which is currently under consideration for publication in the Astrophysical Journal.

THE ASTROPHYSICAL JOURNAL, 401:574–583, 1992 December 20

THE LOW FILLING FACTOR OF DUST IN THE GALAXY

JAYANT MURTHY,[1] H. J. WALKER,[2,3] AND R. C. HENRY[1]
Received 1992 March 4; accepted 1992 June 23

ABSTRACT

We have examined the neighborhood of 745 luminous stars in the *IRAS* Skyflux plates for the presence of dust heated by the nearby star. This dust may be distinguished from the ubiquitous cool cirrus by its higher temperature and thus enhanced 60 μm emission. We have found 123 dust clouds around only 106 of the stars with a volume filling factor of 0.006 and an intercloud separation of 46 pc. Nowhere do we find a region where the dust is smoothly distributed through the volume of space heated by the star and hence we place an upper limit of 0.05 cm^{-3} on the equivalent gas density in the intercloud regions. From the lack of infrared emission near the star, we find that less than 1% of the stellar luminosity is reprocessed within 10 pc of the star.

The clouds, themselves, have an average density of 0.22 cm^{-3} (assuming a standard gas-to-dust ratio) and a radius of 1.9 pc, albeit with wide variations in their properties. We have tentatively identified these clouds with the warm, ionized medium of McKee & Ostriker. We have found two different scale heights of 140 and 540 pc for the number of clouds around different groups of stars which we have interpreted as evidence for different distributions of dust in and out of the Galactic disk. The dust at higher altitudes also appears to be more uniformly distributed with Galactic latitude.

Subject headings: dust, extinction — ISM: general — reflection nebulae

1. INTRODUCTION

One of the major achievements of the *Infrared Astronomical Satellite* (*IRAS*) was its survey of 96% of the sky in four wavelength bands centered at 12, 25, 60, and 100 μm (for details see the *IRAS* Explanatory Supplement 1986). By far the most dominant component seen at 100 μm is emission from the cirrus (Low et al. 1984), dust that is heated by the interstellar radiation field (ISRF); detailed surveys of the dust in our Galaxy, similar to the H I surveys (e.g., Heiles 1975), can be made (see, for example, Boulanger & Perault 1988).

In this work, we have used the *IRAS* Skyflux plates to study the environment in the vicinity of 745 luminous stars. Dust near these stars will be heated by the stellar radiation field to higher temperatures than the cool cirrus, from which it may be distinguished by an enhanced 61/100 μm flux density ratio. Conversely, if there is no emission near these stars, or only emission from the cool cirrus along the line of sight, we may place limits on the amount of dust and, by extension, on the amount of matter near those stars. As the distances to the stars in our program are known (or can be estimated), the dust distribution around those stars provides a probe of the three-dimensional structure of the interstellar medium (ISM) in our Galaxy.

We have found dust clouds around 106 of the 745 stars in our survey for a number fraction of 0.14 ± 0.05, slightly less than, but still consistent with, the value of 0.2 ± 0.11 found by Van Buren (1989) for a smaller sample of stars near the Galactic plane. However, many of these clouds occupy only a small fraction of the total volume around each star, implying a much lower volume filling factor. We will reserve discussion of the individual clouds for a future paper, here discussing only the environment of the stars and its implications for the global morphology of the dust.

[1] Department of Physics and Astronomy, Johns Hopkins University, Baltimore, MD 21218.
[2] SETI Institute, 2035 Landings Drive, Mountain View, CA 94043.
[3] Rutherford Appleton Laboratory, Chilton, Didcot, Oxon, UK.

2. DATA ANALYSIS

As mentioned above, we have examined the *IRAS* Skyflux plates, which are binned in 2′ pixels with an effective resolution of 6′ at all four wavelengths, in the neighborhood of 745 stars, selected primarily from the Bright Star Catalog (Hoffleit 1982). All of the O and B stars in the Bright Star Catalog have been selected and, in addition, all stars of luminosity class I were also examined. Finally, we added all the O stars in the SKYMAP data base (Gottleib 1978). Several regions (Table 1) were excluded from our analysis, including regions within 10° of the Galactic plane, where background subtraction become problematic, and several regions of known molecular cloud concentrations, such as Orion or Taurus. (These regions are identical to those excluded by Boulanger & Perault 1988.) The distribution of our target stars in galactic coordinates is shown in Figure 1. The spectral type, apparent magnitude, and observed $B-V$ for each star were obtained from the Bright Star Catalog; the absolute magnitude, temperaure, and intrinsic $B-V$ were read from tables in Zombeck (1982); and the $E(B-V)$, spectroscopic distance, and luminosity of the star were calculated from the other quantities.

Although virtually all of the emission in the *IRAS* Skyflux plates is due to dust (interplanetary, circumstellar, or interstellar), we are interested in only that part which is actually due to dust heated by the star in question. The remainder, consisting primarily of zodiacal light and the cool cirrus, must therefore be identified and subtracted. We attempted to develop an automated computer procedure to do this but found that, in practice, we were limited to removing only the smooth component of the background, leaving behind any discrete structures, whether associated with the star or not. The first step in our procedure was to select a region of typically 6.7 × 6.7 (201 × 201 pixels) centered on the star (this region

TABLE 1

REGIONS EXCLUDED IN OUR SURVEY

Name	Galactic Longitude	Galactic Latitude
Carina	$245 < l < 275$	$-20 < b < -10$
Cepheus	$98 < l < 141$	$10 < b < 22$
Chamaeleon	$290 < l < 305$	$-20 < b < -10$
Galactic plane	$0 < l < 360$	$-10 < b < 10$
LMC	$273 < l < 286$	$-38 < b < -30$
Lupus	$315 < l < 360$	$10 < b < 30$
Ophiuchus	$l < 50$	$10 < b < 20$
Orion	$190 < l < 220$	$-22.5 < b < -10$
Perseus	$150 < l < 170$	$-32.5 < b < -10$

was smaller if the star was near the edge of a plate) and divide it into blocks of 20 × 20 pixels. We then fitted a grid consisting of the minimum values in each of the blocks by a quadratic surface, which formed our estimate of the smooth background contribution to the plate. In order to ensure that the background was not affected by large bright clouds completely filling a block, we rejected any pixels with intensities more than 3 σ over the mean (of all the pixels) and repeated the procedure. An example of our fit is shown in Figure 2. We obtained an estimate of the quality of our fits from the rms deviations in a relatively flux-free region of each plate. The average deviations for our entire sample are 0.14, 0.20, 0.15, and 0.31 MJy sr^{-1} in the 12, 25, 60, and 100 μm bands, respectively, and are on the same order as errors cited by other groups using similar procedures (e.g., Boulanger et al. 1990).

The remaining emission in the plate consists of not only dust clouds heated by the star but also cool cirrus clouds only coincidentally in the same direction as the star, and we must differentiate between the two. Our selection criteria were that the cloud exist as a distinct entity in the 60 μm map (not necessarily centered on the star) and that the 60/100 μm ratio within the cloud increase toward the star. We have found 123 such clouds (Table 2) around 106 stars, ranging in size and brightness from the large, bright (and well-known) clouds around ζ Oph (HD 149757; Van Buren & McCray 1988) and

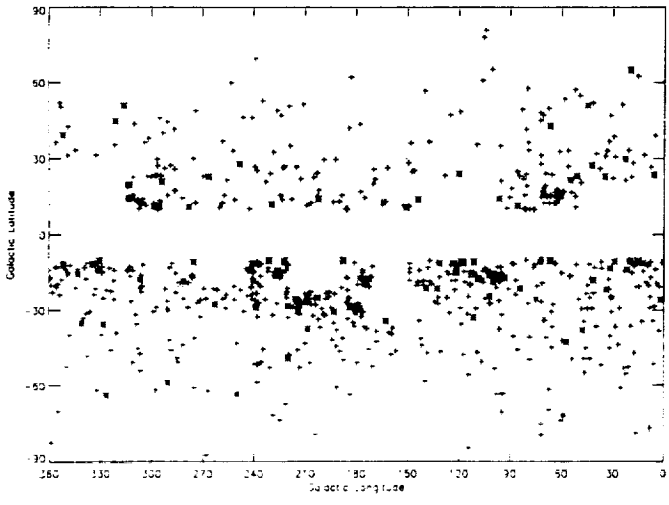

FIG. 1.—The distribution of the stars in our program in Galactic coordinates is shown. Those stars around which we have found dust clouds are plotted as asterisks. Note that we have excluded several regions from consideration, including the Galactic plane, Orion, and Taurus, among others (see Table 1).

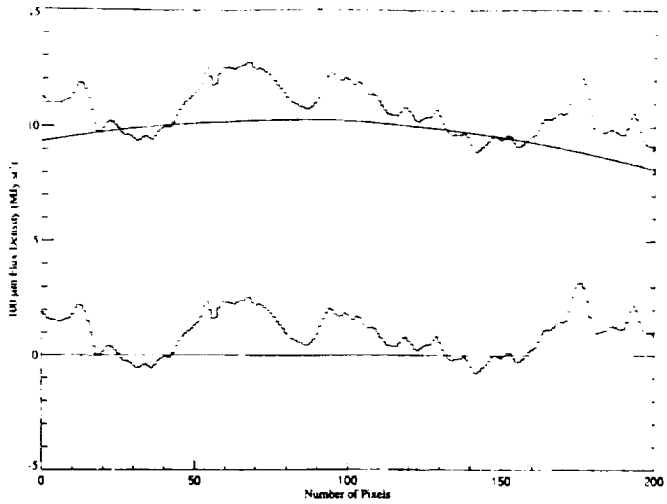

FIG. 2.—A cut through the original Skyflux plate is shown (*upper line*) with our fit to the background emission (*smooth line*). The lower line shows the residual emission. Some of the overall curvature in the original plate has been removed, without affecting the discrete features.

α Cam (HD 30614; de Vries 1985) to those barely distinguishable from the background. In order to estimate the errors in this procedure, we have performed our search twice, with different people, finding agreement in 638 out of the 745 total cases, or in 86% of the cases. This difference is, however, proportionately greater in the number of clouds as 123 clouds were found the first time and 144 the second, with agreement in 67 cases. Not only is there ambiguity in deciding whether a faint path is due to emission from dust heated by the star but there are a significant number of bright features for which it was a subjective decision whether there was an increase in the 60/100 μm ratio toward the star or not. Nevertheless, despite these problems, it is clear that most of the stars in our survey do not have detectable dust clouds nearby.

Selection effects are important in our data and two of them are illustrated in Figure 3, where we have plotted the radius of the clouds as a function of distance from the Sun. The first of these biases is introduced through a finite spatial resolution of the instrument: distant clouds must be larger in order to be above the resolution limit (solid line in Fig. 3). In addition to small clouds not being detected at large distances, the converse effect is also present. This is primarily due to our selection by apparent magnitude: the nearer stars tends to be less intrinsically luminous and thus will not illuminate a large cloud in its entirety. That this is a factor in our results is shown in Figure 4 where we have expressed the radius of the cloud as a fraction of the distance at which the stellar radiation field drops to the level of the ISRF. It should be noticed that the nearby clouds are not significantly smaller, in relation to the stellar luminosity, than those at greater distances. Another consequence of our selection by magnitude is that we automatically discriminate against stars in high obscuration regions where there are more likely to be dust clouds. Finally, as the more luminous stars will both dominate over the ISRF for a larger volume of space and heat dust within that volume to higher temperature, we will be more likely to detect clouds around those stars (Table 3). As a corollary, we will be more likely to observe dust clouds around more distant stars, which tend to be intrinsically brighter, but the clouds will be larger, due to the instrumental resolution.

TABLE 2

STARS WITH DUST CLOUDS

Number (1)	HD (2)	Spectral Type (3)	l (4)	b (5)	V (6)	Distance (pc) (7)	r_c (pc) (8)	d_c (pc) (9)	Density (cm^{-3}) (10)	F_{12} (11)	F_{25} ($\times 10^{-5}$ ergs s^{-1}) (12)	F_{60} ($\times 10^{-5}$ ergs s^{-1}) (13)	F_{100} (14)
1	358	B8I IV	111.7	−32.8	2.1	58	0.1	0.3	8.52	35.3	22.2	3.7	2.5
2	1337	O9 III	117.6	−11.1	6.1	1719	4.5	11.6	1.00	9.1	4.5	3.8	4.9
3	1976	B5 IV	118.7	−10.6	5.6	283	1.7	0.8	1.47	5.1	4.5	4.3	4.9
4	3901	B2 V	121.4	−12.3	4.8	530	1.8	1.6	0.62	7.5	6.0	12.4	6.5
5	4142	B5 V	121.7	−15.0	5.7	215	0.6	0.3	1.70	2.2	2.4	3.3	2.3
6	4180	B5 III	121.8	−14.6	4.5	216	0.7	0.9	2.11	6.4	2.4	2.9	2.8
7	4180	B5 III	121.8	−14.6	4.5	216	0.8	1.0	1.86	6.6	1.3	3.3	3.5
8	4881	B9 V	123.0	−11.3	6.2	108	0.4	0.2	5.48	7.7	4.2	5.0	4.3
9	10144	B3 V	290.8	−58.8	0.5	80	0.2	1.8	3.61	26.2	4.6	1.7	1.3
10	10205	B8 III	132.9	−21.3	4.9	281	0.6	0.3	0.29	3.8	4.8	1.4	0.7
11	10516	B2 V	131.3	−11.3	4.1	341	0.8	3.4	3.37	7.9	4.5	4.0	4.1
12	10516	B2 V	131.3	−11.3	4.1	341	0.9	4.5	5.28	17.7	6.5	4.1	5.5
13	10516	B2 V	131.3	−11.3	4.1	341	0.5	2.7	2.63	23.9	11.3	2.3	1.9
14	13294	B9 V	139.4	−21.3	5.6	85	0.1	0.2	5.48	13.9	7.2	1.5	1.3
15	17098	B9 V	250.3	−63.3	6.4	119	0.2	0.2	1.66	3.9	3.9	1.4	0.8
16	19374	B1 V	163.0	−34.2	6.1	967	3.6	3.5	0.41	10.9	13.3	3.7	3.5
17	24587	B6 V	220.0	−49.1	4.7	138	0.2	0.2	1.67	3.7	1.9	4.0	1.5
18	25204	B3 V	178.4	−29.4	3.5	302	0.9	3.2	7.64	7.4	3.1	5.0	6.6
19	25204	B3 V	178.4	−29.4	3.5	302	0.9	2.5	2.51	10.1	8.3	3.5	3.7
20	25204	B3 V	178.4	−29.4	3.5	302	0.6	1.8	1.76	5.7	2.0	3.0	2.2
21	25330	B5 V	180.8	−30.8	5.7	175	0.6	1.0	20.1	3.0	1.6	2.7	5.2
22	25330	B5 V	180.8	−30.8	5.7	175	0.5	0.7	4.99	9.0	3.1	2.4	3.1
23	26676	B8 V	182.7	−28.4	6.2	227	0.7	0.3	11.1	15.3	11.1	26.0	19.6
24	26912	B3 IV	184.2	−28.9	4.3	532	5.2	3.4	0.88	6.6	2.3	8.8	9.4
25	27742	B8 IV	175.3	−19.7	6.0	290	0.9	0.6	2.78	80.2	7.5	2.5	2.9
26	27778	B3 V	172.8	−17.4	6.4	746	2.4	4.0	6.66	5.0	5.3	4.6	7.6
27	28149	B7 V	174.3	−17.7	5.5	202	1.0	0.4	7.07	17.3	6.7	18.6	16.7
28	28375	B3 V	193.4	−30.6	5.6	765	2.2	1.8	0.52	7.4	4.9	4.6	3.5
29	29365	B8 V	177.9	−17.2	5.9	229	0.7	0.7	29.2	−6.9	5.7	4.0	8.1
30	30614	O9 Ia	144.1	14.0	4.3	966	16.7	7.0	0.07	5.9	6.2	9.9	5.7
31	32343	B2 V	151.0	10.8	5.1	577	2.7	3.8	2.51	14.1	5.0	6.4	7.2
32	32343	B2 V	151.0	10.8	5.1	577	1.4	5.4	5.58	8.0	3.1	3.2	5.0
33	32612	B2 IV	214.3	−30.2	6.4	1626	3.3	5.3	1.16	0.1	4.4	2.9	3.5
34	33328	B2 IV	209.1	−26.7	4.3	616	4.8	2.9	0.12	8.8	1.9	3.8	2.6
35	32686	B5 IV	203.0	−25.0	6.1	348	1.3	1.0	8.01	15.8	3.8	8.8	12.8
36	33949	B9 V	213.9	−27.5	4.4	53	0.2	0.2	10.4	4.7	−1.4	3.2	3.3
37	34085	B8 Ia	209.2	−25.2	0.1	222	1.1	5.1	1.48	11.4	6.5	4.3	4.2
38	34085	B8 Ia	209.2	−25.2	0.1	222	1.0	2.3	0.28	7.2	0.8	4.1	2.0
39	34085	B8 Ia	209.2	−25.2	0.1	222	1.2	5.7	1.57	9.2	8.1	4.4	4.8
40	34085	B8 Ia	209.2	−25.2	0.1	222	0.7	7.0	5.96	12.2	8.0	3.9	5.2
41	34085	B8 Ia	209.2	−25.2	0.1	222	1.0	6.6	2.73	10.9	3.6	3.3	4.1
42	34085	B8 Ia	209.2	−25.2	0.1	222	0.8	7.1	23.8	43.6	16.0	15.0	20.1
43	34798	B3 V	220.3	−28.4	6.4	1214	2.1	2.7	0.65	1.7	0.5	1.1	1.3
44	34816	B0 IV	214.8	−26.2	4.3	649	1.3	10.1	4.68	9.5	6.3	2.1	3.4
45	35337	B2 IV	216.0	−25.7	5.2	996	2.9	7.8	2.55	5.9	3.1	2.2	3.8
46	35532	B2 Vn	188.0	−10.3	6.2	989	5.7	2.9	0.25	7.9	3.9	4.1	3.6
47	37795	B7 IV	238.8	−28.9	2.6	76	0.1	0.3	1.94	5.5	1.3	1.5	0.9
48	42933	B3 III	263.3	−27.7	4.8	998	5.2	2.0	0.08	3.8	3.0	3.7	2.2
49	43955	B2 V	227.5	−16.1	5.5	818	1.7	4.3	1.44	3.9	1.0	1.4	1.8
50	44743	B1 II	226.1	−14.3	2.0	308	3.7	7.1	0.44	6.9	4.0	3.6	3.7
51	46064	B1 V	222.4	−10.5	6.2	1034	3.3	3.4	0.42	4.6	2.7	2.8	2.5
52	49333	B7 III	231.4	−10.3	6.1	541	1.6	0.8	1.33	13.9	3.7	3.1	3.3
53	50013	B1 IV	242.4	−14.5	4.0	557	1.3	9.6	9.03	5.7	5.0	2.5	4.8
54	58050	B2 V	202.5	14.2	6.4	1233	3.4	5.5	1.01	4.2	7.7	1.5	2.4
55	67159	B9 V	230.0	12.1	6.2	121	0.2	0.2	17.9	2.7	2.8	1.4	2.0
56	68520	B6 IV	281.6	−18.6	4.3	161	0.3	0.6	7.10	6.4	2.7	2.8	2.9
57	74375	B1 II	275.8	−10.9	4.3	635	8.8	7.6	0.29	6.4	2.7	3.4	4.5
58	83754	B5 V	248.7	27.8	5.1	169	0.5	0.4	0.68	4.9	2.4	1.6	1.2
59	83754	B5 V	248.7	27.8	5.1	169	0.5	0.5	1.44	2.9	2.3	1.4	1.3
60	89353	B9 Ib	266.8	22.9	5.3	806	1.4	1.2	0.18	92.7	8.7	1.3	0.8
61	91355	B9	278.6	11.1	5.7	108	0.2	0.2	28.9	5.7	0.5	2.6	4.1
62	91356	B4	278.6	11.1	6.1	215	0.3	0.9	26.0	5.5	0.8	2.7	4.3
63	105383	B9 V	296.0	11.5	6.4	125	0.5	0.2	3.57	19.0	11.3	8.0	5.8
64	105521	B3 IV	294.4	20.9	5.5	935	1.9	4.3	3.15	4.9	2.4	3.5	4.7
65	105521	B3 IV	294.4	20.9	5.5	935	2.4	2.3	0.47	7.1	4.2	4.0	3.0
66	108257	B3 V	299.0	11.2	4.8	580	4.8	2.5	0.87	4.0	2.5	6.1	6.5
67	116658	B1 III	316.1	50.8	1.0	162	0.8	1.9	0.25	8.6	8.8	5.8	2.3
68	119361	B8 III	313.2	19.8	6.0	447	1.2	0.9	1.78	6.4	4.5	1.6	2.2
69	119605	G0 Ib	321.0	44.8	5.6	816	1.4	0.8	0.92	3.2	3.6	1.4	1.5

TABLE 2—*Continued*

Number (1)	HD (2)	Spectral Type (3)	l (4)	b (5)	V (6)	Distance (pc) (7)	r_c (pc) (8)	d_c (pc) (9)	Density (cm^{-3}) (10)	F_{12} (11)	F_{25} ($\times 10^{-5}$ ergs s^{-1}) (12)	F_{60} (13)	F_{100} (14)
70	120307	B2 IV	314.4	19.9	3.4	433	0.9	3.6	0.97	4.4	2.7	2.5	2.0
71	120307	B2 IV	314.4	19.9	3.4	433	1.1	3.0	0.40	4.4	1.9	2.7	1.9
72	120640	B2 V	313.5	14.7	5.8	892	2.9	4.7	1.50	7.1	4.3	3.4	4.7
73	121263	B2 IV	314.1	14.2	2.5	291	1.1	5.3	2.97	11.8	6.8	4.3	5.0
74	124771	B4 V	306.9	−18.0	5.1	155	0.8	0.4	3.75	3.1	4.3	9.5	7.2
75	128220	O7 III	20.1	64.9	8.5	3158	8.2	7.1	0.06	5.6	3.8	1.7	1.3
76	135742	B8 V	352.0	39.2	2.6	54	0.1	0.2	3.96	12.9	6.5	2.3	1.5
77	141527	G0 I	45.1	51.0	5.8	3526	8.1	1.6	0.06	66.3	10.0	1.9	1.2
78	149630	B9 V	66.9	42.7	4.2	43	0.0	0.2	5.93	6.3	2.7	0.9	0.5
79	149757	O9 V	6.3	23.6	2.6	168	1.0	7.9	10.8	19.4	14.6	15.3	20.7
80	151525	B9	22.9	29.8	5.2	71	0.1	0.2	20.8	5.9	34.9	1.8	2.3
81	153261	B2 IV	330.7	−10.3	6.1	1135	2.0	5.4	2.47	8.8	4.4	3.2	3.9
82	157246	B1 I	334.6	−11.5	3.3	688	3.0	9.8	0.91	7.8	7.9	6.1	6.4
83	157246	B1 I	334.6	−11.5	3.3	688	3.6	13.1	1.70	10.7	6.3	6.5	9.0
84	158148	B5 V	42.7	27.3	5.5	205	0.4	0.7	7.25	21.7	14.8	1.1	1.5
85	159082	B9 V	35.0	22.9	6.4	121	0.3	0.2	10.6	6.3	2.4	2.5	3.0
86	163506	F2 Ib	51.4	23.2	5.5	1111	3.5	0.3	0.14	114.5	35.8	4.8	2.1
87	166014	B9 V	55.2	21.6	3.8	37	0.0	0.2	10.4	3.3	3.5	1.3	1.0
88	167257	B9 V	343.1	−15.7	6.1	110	0.2	0.2	4.92	7.5	5.9	2.0	1.8
89	167756	B0 Ia	351.5	−12.3	6.3	3301	10.5	15.4	0.27	9.5	7.7	5.8	5.9
90	172958	B8 V	60.8	15.7	6.4	282	0.5	0.3	2.96	−1.3	−0.2	1.8	1.7
91	175360	B8	12.5	−11.3	5.9	220	0.8	0.2	0.95	34.8	18.8	5.0	3.4
92	175876	O6	15.3	−10.6	6.9	2741	9.6	5.3	0.08	75.5	43.4	10.2	5.3
93	176502	B3 V	70.9	16.0	6.2	1138	3.0	3.3	1.14	2.3	1.1	2.2	3.0
94	177817	B8 IV	20.0	−10.7	6.0	327	0.8	0.4	1.82	19.0	15.5	5.0	4.1
95	181615	B2 V	21.8	−13.8	4.6	356	0.7	1.7	1.41	174.7	31.6	5.1	2.7
96	181858	B3 IV	29.1	−10.6	6.7	1524	2.8	1.9	0.17	6.5	5.4	2.7	1.7
97	184915	B0 II	31.8	−13.3	4.9	689	1.4	7.5	2.41	8.5	10.5	3.5	3.8
98	186042	B8	2.1	−25.9	6.2	234	0.5	0.5	8.11	1.5	0.0	2.4	3.5
99	189775	B5 III	86.0	11.5	6.2	541	0.9	0.9	3.55	106.1	16.7	3.6	3.5
100	191639	B1 V	34.0	−21.7	6.5	1204	2.9	2.6	0.20	7.1	8.6	2.7	1.9
101	191692	B9 II	41.6	−18.1	3.2	46	0.2	0.4	48.3	12.8	11.7	3.9	6.7
102	193924	B2 IV	340.9	−35.2	1.9	213	0.4	3.9	3.19	9.3	7.1	2.6	2.3
103	193964	B9 V	96.5	14.4	5.7	92	0.2	0.2	5.10	3.7	0.5	1.7	1.4
104	196519	B9 III	328.4	−35.6	5.2	109	0.2	0.2	4.67	3.0	3.2	2.0	1.9
105	196740	B5 IV	67.0	−10.3	5.0	228	0.7	0.7	2.41	4.1	2.5	3.0	3.1
106	199140	B2 IIIv	72.8	−10.5	6.6	1858	4.3	2.0	0.07	4.0	1.8	4.0	1.8
107	204867	G0 Ib	48.0	−37.9	2.9	229	0.5	0.8	2.04	4.2	5.4	1.7	1.8
108	209409	B7 IV	57.4	−42.7	4.7	178	0.5	0.5	1.77	6.0	6.1	2.7	2.3
109	209833	B9 V	84.5	−21.3	5.6	89	0.2	0.2	16.3	2.9	1.8	2.0	2.8
110	212710	B9 V	120.2	24.1	5.3	73	0.1	0.3	76.3	1.8	2.4	0.8	1.7
111	212883	B2 V	93.6	−17.0	6.5	1172	3.1	1.0	0.5	4.1	7.5	3.5	1.3
112	214168	B2 V	96.4	−16.1	5.7	863	4.1	3.2	0.44	5.0	2.5	4.4	4.2
113	214680	O9 V	96.7	−17.0	4.9	769	2.7	6.2	0.49	8.9	4.0	4.0	3.6
114	214680	O9 V	96.7	−17.0	4.9	769	1.7	6.3	1.09	5.1	4.6	3.8	3.5
115	214993	B2 III	97.7	−16.2	5.2	1031	3.6	3.9	0.24	9.8	4.7	4.1	3.2
116	216200	B3 IV	100.0	−15.5	5.9	917	1.9	4.7	2.46	2.5	2.0	1.7	2.5
117	217101	B2 IV	100.1	−18.5	6.2	1399	4.5	3.9	0.44	8.2	3.7	5.3	4.7
118	217675	B6 III	102.2	−16.1	3.6	148	1.0	0.6	1.83	7.2	3.4	9.0	6.4
119	217811	B2 V	103.1	−14.6	6.4	937	2.8	3.1	0.51	3.8	5.5	2.8	2.6
120	219927	B8 III	102.3	−24.4	6.3	523	1.2	0.6	0.93	5.8	4.9	2.7	2.3
121	222173	B8 V	109.0	−17.6	4.3	116	0.3	0.3	2.79	4.9	4.5	1.6	1.5
122	222304	B9 V	111.3	−10.8	5.3	77	0.2	0.2	13.49	4.7	1.6	1.2	1.7
123	223145	B3 V	326.6	−63.9	5.2	737	1.5	1.9	0.30	4.9	1.9	1.4	1.1

NOTES.—Col. (7) is the spectroscopic distance of the star from the Sun. Cols. (8) and (9) are, respectively, the distance of the cloud from the star, as defined by the average 60/100 μm ratio in the cloud (see text), and the average radius of the cloud, assuming a spherical cloud. Col. (10) is the average density in the cloud using the 100 μm flux density. Cols. (11) through (14) are, respectively, the average 12, 25, 60, and 100 μm flux densities of the cloud.

In order to model the emission from the dust near the star, or to place upper limits on the amount present, we simply set equal the heat input from the star into the dust, calculated using a Kurucz model (Kurucz 1979) of the appropriate temperature multiplied by a dust absorption profile from Draine & Lee (1984), and the radiation emitted by the dust as a function of the dust temperature, again using optical constants from Draine & Lee. The predicted signal in each of the *IRAS* bands was found by convolving the calculated dust emission profile with the instrument response function. In Figure 5, we have plotted the expected emission at 100 μm from stars of several spectral types placed in a uniformly distributed medium of density 0.1 cm^{-3} as a function of distance from the star. (The density of the dust is quoted here, and elsewhere in this work, in terms of the equivalent amount of H I, assuming the canonical gas to dust ratio of 5.8×10^{21} atoms cm^{-3} mag^{-1}; Bohlin, Savage, & Drake 1978. Note that this is implicit in the Draine & Lee model.)

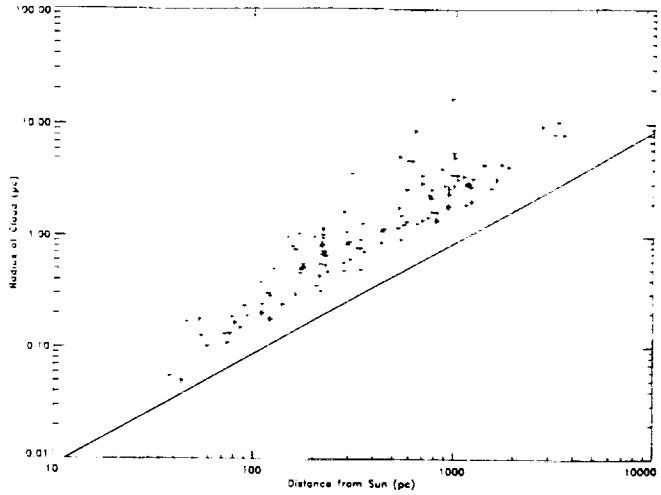

FIG. 3.—The radius of each of our clouds is plotted as a function of distance from the Sun. Clouds which fell below the solid line cannot be detected in our survey because of the finite spatial resolution of the instrument. In addition, large clouds near the Sun are not detected because the nearby stars are, in general, too intrinsically faint to illuminate large clouds in their entirety.

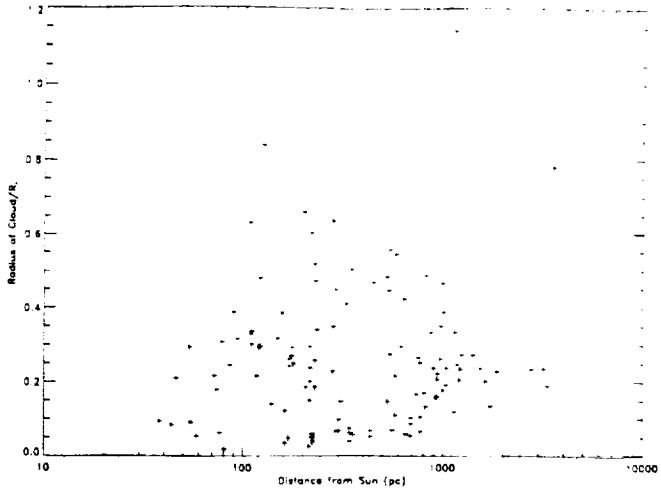

FIG. 4.—The radius of the cloud divided by the distance at which the stellar heating drops to the level of the ISRF (R_s) is plotted against distance from the Sun. From this plot, we see that the tendency for the nearby detected clouds to be smaller is probably due to the lower luminosities of the closer stars and thus is an observational artifact.

3. RESULTS AND DISCUSSION

3.1. *Cloud Properties*

In the present work, we are concerned only with the group properties of the cloud listed in Table 2 and so have used several approximations to characterize them. We have assumed spherical clouds with a radius given by the average length over two orthogonal axes (defined by the plate in question) at a distance from the exciting star such that the predicted 60/100 μm ratio is equal to the observed value (defined as the average over the entire cloud). The amount of dust in each cloud was estimated by calculating an emissivity per grain based on the ratio of the 60/100 μm emission in each pixel, dividing into the observed emission in that pixel, and summing over all the pixels in the cloud. Finally, the average density in the cloud was obtained by dividing by the volume.

We have tabulated the average properties of the detected clouds in Table 4. We find an average cloud radius of 1.9 pc and an average (equivalent H I) density of 0.2 cm^{-3}. However, there is a wide variation in cloud sizes and most have a radius of less than 0.5 pc and a density of less than 0.05 cm^{-3}, as may be seen from the histograms in Figures 6 and 7. The column density through one of these clouds is typically less than about 10^{19} cm^{-2}. Their properties are strongly reminiscent of the warm clouds (warm, ionized medium) in the McKee & Ostriker (1977) theory, of which one example may be the local cloud around our Sun (Bruhweiler & Vidal-Madjar 1987).

We can calculate an average intercioud distance by noting that the total volume of space probed in our program is 6.3×10^6 pc^3, where the volume probed by a star is defined to be that region in which the stellar radiation field exceeds the interstellar value. As we detect 123 clouds in this volume, this implies that there is one cloud per 5.1×10^4 pc^3 or that there is an average of 46 pc between clouds. This is much larger than the intercloud distance of 12 pc (for the warm, ionized clouds) in McKee & Ostriker (1977). The total volume of space occupied by our clouds if 4×10^4 pc^3 leading to a filling factor of 0.006, much lower than the 0.23 in the McKee-Ostriker theory.

This is a very low filling factor, and it is important that we understand both what we are measuring and the uncertainties in our procedure. Unfortunately, because of our observational biases, we do not sample a complete cloud distributed at any point and it is difficult for us to estimate by how much we

TABLE 4

CLOUD PROPERTIES

Parameter	Value
Total number of clouds	123
Total volume of clouds	4.3×10^4 pc^3
Total number of atoms	2.8×10^{59} atoms
Average density	0.22 cm^{-3}
Total volume probed	6.3×10^6 pc^3
Total radiation emitted by clouds	3.7×10^{36} ergs s^{-1}
Total stellar radiation	4.0×10^{40} ergs s^{-1}
Average cloud radius	1.9 pc
Average cloud distance from star	2.8 pc

TABLE 3

STELLAR LUMINOSITY EFFECTS

Parameter	$L_* < 10^{37}$ ergs s^{-1}	$L_* > 10^{37}$ ergs s^{-1}
Number of stars	550	195
Number of stars heating dust	52	54
Number of clouds	55	68
Fraction of stars heating dust	0.09	0.28
Average number of clouds per star	1.06	1.26
Average cloud radius (pc)	0.59	2.99

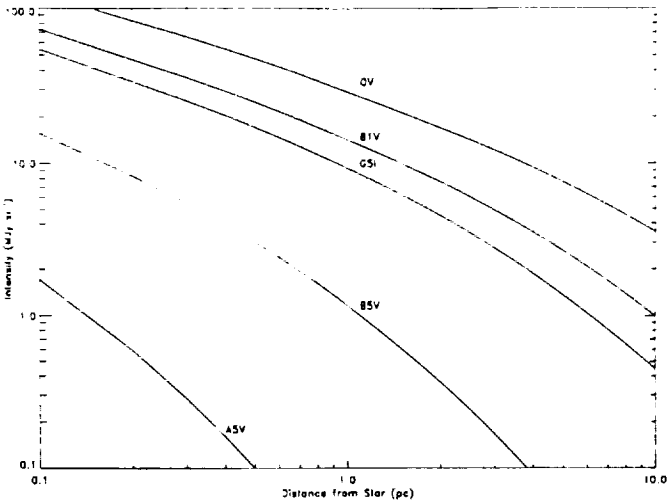

FIG. 5.—The emission seen from the dust at the given distance from the star is plotted for several different spectral types, assuming a uniform dust distribution of density 0.1 cm^{-3}. The radiation field from a hot star may light up dust clouds for many parsecs around.

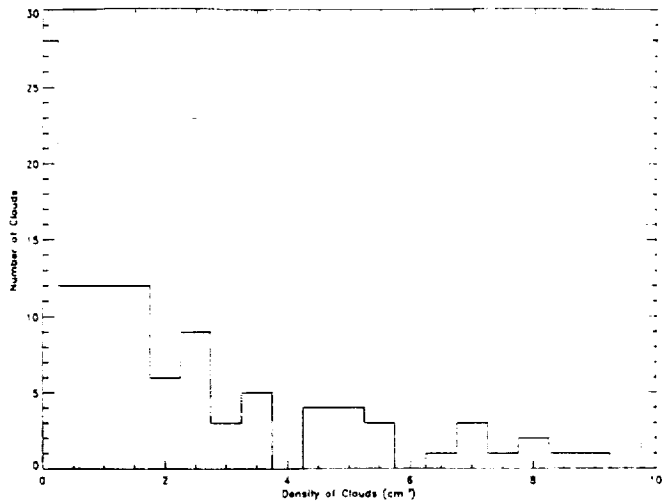

FIG. 7.—A histogram of the density of the clouds is plotted in 0.5 cm^{-3} bins. The distribution is heavily weighted to less dense clouds. The last bin contains all densities of 10 cm^{-3} or higher.

undercount the number of clouds. The average distance between clouds is dependent only on the inverse cube root of the number of clouds and is thus relatively robust; however, the filling factor is dependent on the total volume of the clouds and thus may be in error by a considerable amount, although it is difficult to imagine that we are missing over 95% of the warm material. Our data are not consistent with the conclusion of Kulkarni & Heiles (1987), based on a number of Hα measurements (see Reynolds 1990a), that the filling factor of the warm gas was 0.5 and the filling factor of the warm, ionized medium (WIM) was 0.11, unless the special environment we are probing has been cleared of dust by the stars themselves.

Considering our selection effects, it is difficult to know just which parameter is a true estimator of the cloud distribution and, pending further modeling, we have chosen to use the fraction of stars in our survey which heat nearby dust as our estimator. In the interest of less involved sentences, we will hereafter refer to this quantity as simply the fraction of stars with dust.

The latitude dependence of the fraction of stars heating dust is tabulated in Table 5 and illustrated in Figure 8 (plus signs). This dependence is fitted reasonably well by a cosecant law (*solid line*) except at the highest latitudes, where the sample size is small. If, however, we break the stars into groups, based on intrinsic luminosity, we find that only the less luminous stars (asterisks in Fig. 8) follow a cosecant law. Not only do a greater fraction of the bright stars heat nearby clouds (diamonds in Fig. 8; cf. Table 3), but the distribution falls of much more slowly with increasing Galactic latitude, perhaps reflecting a more uniform distribution of dust once out of the plane of the Galaxy. It should be cautioned that a much more rigorous approach, including Monte Carlo simulations of the cloud dis-

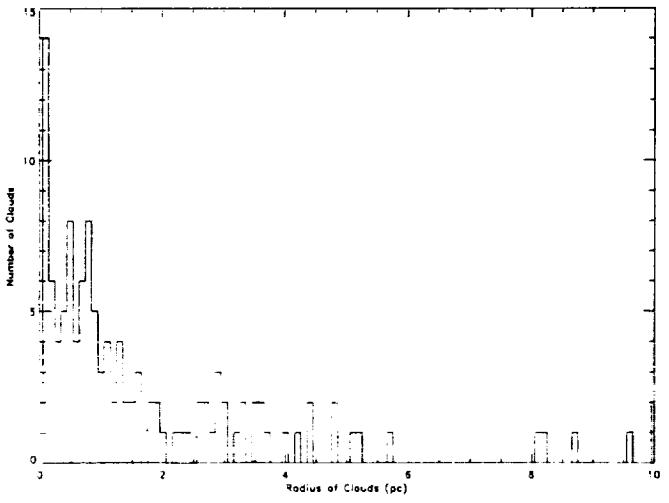

FIG. 6.—A histogram of the number of clouds as a function of radius is plotted. The bin size is 0.1 pc and the last bin contains all clouds of radius 10 pc or greater. Despite the spatial resolution of the instrument, which places a stringent lower limit on the size of a cloud which can be detected (depending on distance), this distribution is heavily peaked to smaller clouds.

TABLE 5

DISTRIBUTION OF CLOUDS WITH LATITUDE

Latitutde Range	Total Number of Stars	Number of Stars with Dust	Fraction of Stars with Dust
$\|b\| > 50$	79	6	0.076
$40 < \|b\| < 50$	71	4	0.056
$30 < \|b\| < 40$	92	9	0.098
$20 < \|b\| < 30$	203	28	0.138
$10 < \|b\| < 20$	300	59	0.197
Stars of $L_* < 10^{37}$ ergs s^{-1}			
$\|b\| > 50$	67	1	0.015
$40 < \|b\| < 50$	62	4	0.065
$30 < \|b\| < 40$	74	5	0.068
$20 < \|b\| < 30$	164	16	0.098
$10 < \|b\| < 20$	183	26	0.142
Stars of $L_* < 10^{37}$ ergs s^{-1}			
$\|b\| > 50$	12	5	0.417
$40 < \|b\| < 50$	9	0	0
$30 < \|b\| < 40$	18	4	0.222
$20 < \|b\| < 30$	39	12	0.308
$10 < \|b\| < 20$	117	33	0.282

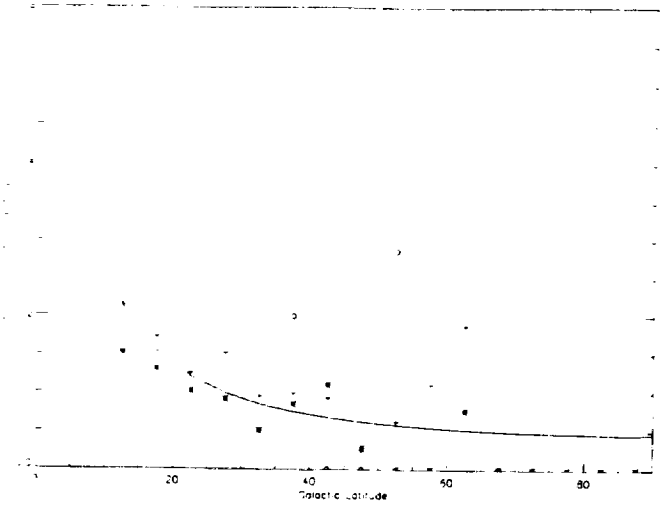

FIG. 8.—The fraction of stars heating nearby dust clouds is plotted as a function of latitude (*plus signs*). The distribution is fitted reasonably well by a cosecant law (*solid line*). We have divided the stars into two groups based on whether their luminosity was less than or greater than 10^{37} ergs s^{-1} and plotted the latitude dependence of the clouds around each group of stars as asterisks and diamonds, respectively. Although the clouds around the less luminous stars (which lie largely in the Galactic plane) still are consistent with a cosecant law, the clouds around the brighter stars appear to follow a much flatter distribution, albeit with poorer statistics, perhaps indicating a more uniform distribution of dust away from the plane.

tributions, will be necessary to ensure that our results are not simply due to selection effects.

The z dependence of the clouds is listed in Table 6 and plotted in Figure 9. The luminosity effects completely mask the relation with height above the Galactic plane for the entire sample, as the fraction of intrinsically bright stars increases

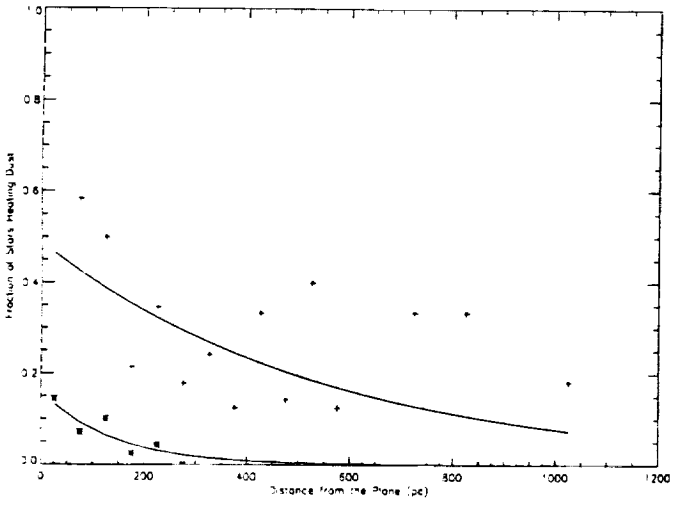

FIG. 9.—The z dependence of the fraction of stars with clouds is plotted for stars with a luminosity less than 10^{37} ergs s^{-1} (*asterisks*) and for those with a greater luminosity (*plus signs*). The two groups follow different distributions and the best-fit (arbitrarily weighting each point by the square root of the number of stars in that bin) exponential distributions to each (*solid lines*) have scale heights of 140 and 540 pc, respectively. This may reflect two populations of dust, one in the plane of the Galaxy (where the cooler stars in our survey tend to lie) and another with a more extended distribution. We detect several clouds at distances of more than 1 kpc from the Galactic plane, more than would be expected even with a scale height of 500 pc from the dust.

TABLE 6

DISTRIBUTION OF CLOUDS WITH HEIGHT ABOVE PLANE

Height above Plane	Total Number of Stars	Number of Stars with Dust	Fraction of Stars Dust
$z < 100$ pc	384	46	0.120
100 pc $< z <$ 200 pc	163	23	0.141
200 pc $< z <$ 300 pc	86	15	0.174
300 pc $< z <$ 400 pc	47	8	0.170
400 pc $< z <$ 500 pc	18	5	0.278
500 pc $< z <$ 1000 pc	36	7	0.194
1000 pc $< z$	11	2	0.182
Stars of $L_* < 10^{37}$ ergs s^{-1}			
$z < 100$ pc	370	39	0.105
100 pc $< z <$ 200 pc	129	10	0.078
200 pc $< z <$ 300 pc	32	1	0.031
300 pc $< z <$ 400 pc	10	0	0.000
400 pc $< z <$ 500 pc	2	1	0.500
500 pc $< z <$ 1000 pc	7	1	0.143
1000 pc $< z$	0	0	
Stars of $L_* > 10^{37}$ ergs s^{-1}			
$z < 100$ pc	14	7	0.500
100 pc $< z <$ 200 pc	34	13	0.382
200 pc $< z <$ 300 pc	54	14	0.259
300 pc $< z <$ 400 pc	37	8	0.216
400 pc $< z <$ 500 pc	16	4	0.250
500 pc $< z <$ 1000 pc	29	6	0.207
1000 pc $< z$	11	2	0.182

with distance, and we have plotted only the fraction of stars with dust for the two luminosity subdivisions in the figure. Aside from the normalization, we find exponential scale heights of 540 pc for the fraction of luminous stars with dust and 140 pc for the less luminous stars, consistent with the idea of two different distributions being sampled by the different stars. These values are comparable to the scale heights of 100–500 pc found from surveys of H I (Lockman, Hobbs, & Shull 1986) and cold cirrus (Burton et al. 1986). There are, however, significantly more clouds far from the plane than would be expected from even a 500 pc scale height, perhaps due to radiation pressure from Galactic plane stars (Franco et al. 1991).

It is difficult to compare these results directly with other studies of the distribution of interstellar matter, either from observations of the gas, namely H I (e.g., Heiles 1976; Burstein & Heiles 1978) and CO (e.g., Sanders, Scoville, & Solomon 1985), or from observations of the dust (e.g., Knude 1979; Feitzinger & Stuwe 1986), because of the very different method and selection effects involved. It is not obvious that the different methods will even select the same population of clouds; the giant molecular clouds (GMCs) of Sanders et al. are obviously a very different population from our sample. We are probing the environment near a number of luminous stars where the dust, and presumably the gas, will be heated by the radiation field of the star and we have tentatively identified our clouds as part of the WIM of McKee & Ostriker (1977), which will be essentially undetectable by, at least, radio observations. Conversely the other methods probe the general ISM and tend to be more sensitive to the cold, neutral medium (CNM).

On the other hand, the low densities in our clouds are similar to the 0.02 cm^{-3} for the average cloud of Knude (1981) from *uvbyβ* photometry of A and F stars. Knude also found a lower limit of 0.7 pc for his distribution of cloud sizes which he hypothesized as either a selection effect or a true lower limit

below which clouds evaporated rapidly. Many of our clouds are, in fact, smaller than this value even though the environment near the luminous stars of our survey is likely to be harsher than the region probed by Knude and hence it seems likely that the lower limit was indeed a selection effect.

Feitzinger & Stuwe (1986), using a complete and uniform set of dark clouds, derived the number density of dark clouds, presumably representing the CNM, to be 8×10^{-5} pc^{-3} within 250 pc of the Sun dropping to 10^{-5} pc^{-3} within 500 pc^{-3} (and to 10^{-6} pc^{-3} within 1000 pc). We obtain a value of 2×10^{-5} pc^{-3} within 200 pc of the Sun for our diffuse clouds, perhaps indicating that the warm, diffuse clouds we sample are less numerous than the colder variety. Again, we will have to examine our selection effects carefully before drawing firm conclusions.

3.2. *Gas Densities*

Probably one of the most important and secure results in this work is the low density around our program stars. We have calculated the density in a series of concentric circles around each of the 745 stars assuming that all the emission above the background at 60 μm is due to thermal emission from dust uniformly distributed around the star, with optical constants from Draine & Lee (1984). An associated error for each point was calculated using the rms deviations of the background in the respective plate, and a weighted average over all the stars was derived (Fig. 10). (It is important to realize that what we call the density is, strictly, not the actual density but is instead an upper limit, including the effects of cool cirrus spatially distant from the star.) The density we derive around each star depends on both the amount of emission nearby and on the strength of the stellar radiation field while the σ's of the density depend on the rms error of the appropriate plate (essentially the same for all the plates), and on the stellar luminosity. Thus the errors will be least near the brightest stars, and the average density will be dominated by the densities near those stars. Most of the contribution to this average comes from two stars (ζ Oph and Spica) for which there is enough

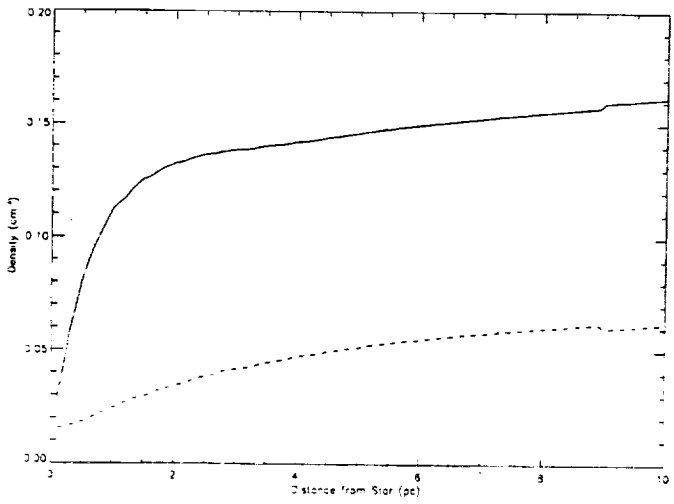

FIG. 10.—The upper limits on the density (using the 60 μm data) near each of the stars have been weighted by the appropriate error bars and summed to yield an average upper limit on the density as a function of distance from the star (*solid line*). This density is heavily weighted by two stars (ζ Oph and Spica), both of which have nearby dust clouds, and if we exclude them, we find a much lower average upper limit of 0.05 cm^{-3} (*dashed line*).

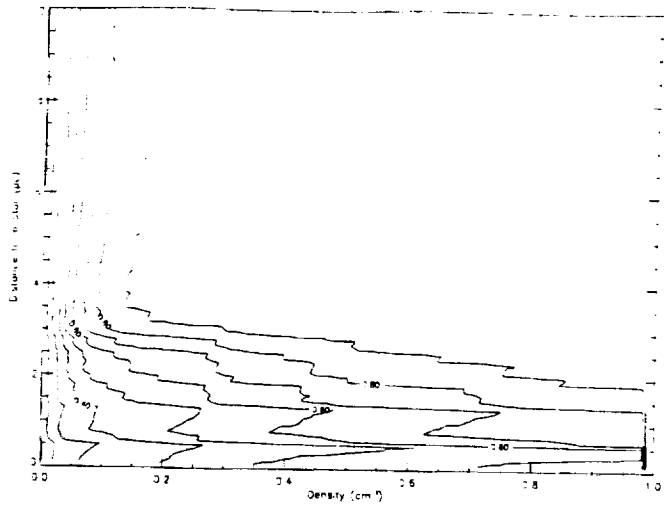

FIG. 11.—Another view of the low densities near the stars in our survey is to show the fraction of stars with densities below the given value. The change in the slope of the contours is caused by our including only stars for which the heat input into the dust exceeds the interstellar value and thus, as we probe farther away from the star, only the most luminous stars—which have better upper limits—are included. At 5 pc from the star, we see that the upper limit on the gas density is less than 0.05 cm^{-3} for about 50% of the stars and less than 0.1 cm^{-3} for about 80% of the stars (including those stars with dust clouds detected nearby).

emission at 60 μm combined with a strong enough stellar radiation field that they dominate the density and, if we exclude these two stars, the upper limit on the density drops from about 0.12 cm^{-3} to 0.05 cm^{-3} (*dashed line*).

Another view of this information is presented in Figure 11 where we have plotted the fraction of stars with a density lower than the abscissa in a volume of radius given by the ordinate; for example, the density of the matter within 6 pc of the central star is less than 0.1 cm^{-3} for 80% of the stars. The shape of the contours in the figure are an artifact of our processing; as the distance from the star increases, we only use those stars for which the stellar radiation field is greater than the ISRF. Thus, at large distances from the central star, we are probing only intrinsically bright stars which will, as discussed above, have more restrictive limits on the amount of nearby dust. If we were to consider only those bright stars, the contours in Figure 11 would be even more restrictive near the star, emphasizing the paucity of dust in our survey.

The exact value of the density is independent on several of our assumptions. The albedo in our model is near 0.5, as given by Draine & Lee (1984). There is, however, evidence that the grains are actually much blacker in the far-ultraviolet (Murthy, Henry, & Holberg 1991; Hurwitz, Bowyer, & Martin 1991) which would drive the densities to even lower values. It has become clear from many studies (see Desert, Boulanger, & Puget 1990 for a summary and references) that a significant part of the 60 μm emission arises from transient heating of small grains, which comprise only a small part of the entire dust population by mass. The Draine & Lee (1984) model does not include this emission and thus the actual density should again be lower. We have also assumed that there is no contribution to the heating from photons below 912 Å, perhaps not true for the low densities found in this work. On the other hand, we have ignored extinction by whatever material is between the star and the point under consideration which would lower the radiation field and thus the heating at that

point, increasing the derived density. Finally, the derived gas density depends on the assumed value of the gas-to-dust ratio. We have used a constant ratio of 5.8×10^{21} atoms cm^{-3} mag^{-1} Bohlin et al. 1978); however, there are strong indications that this value, in fact, varies by at least a factor of 4 in different directions (Burstein & Heiles 1978) and may vary even more near the luminous stars in our study.

A related issue is the amount of stellar energy which escapes the immediate vicinity of the star and contributes to the ionization and energetics of the gas in our Galaxy. The total amount of energy emitted in the *IRAS* bands by all of the dust clouds is 3.7×10^{36} ergs s^{-1} which is 10^{-4} of the total stellar emission. Assuming that about 50% of the total output from the dust is emitted in the *IRAS* bands (Desert et al. 1990), less than 1% of the stellar luminosity is reprocessed near the star, in accord with many other studies of the redistribution of stellar photons. These results are not affected even if we use all of the emissions near the star (Fig. 12), rather than just that part in the clouds identified.

Similar conclusions have been drawn by both Leisawitz & Hauser (1988), who have found, from a study of several OB clusters, that less than 10% of the stellar flux is absorbed within 50 pc of the stars after the stars have moved away from their prenatal molecular clouds, and by Reynolds (1990b) from the high ionization in the local ISM (within 100 pc of the Sun). There are not enough nearby sources to maintain this ionization and therefore UV radiation from O and B stars in the Galactic plane must be reaching the solar neighborhood, implying that there must be paths of low optical depth over that distance.

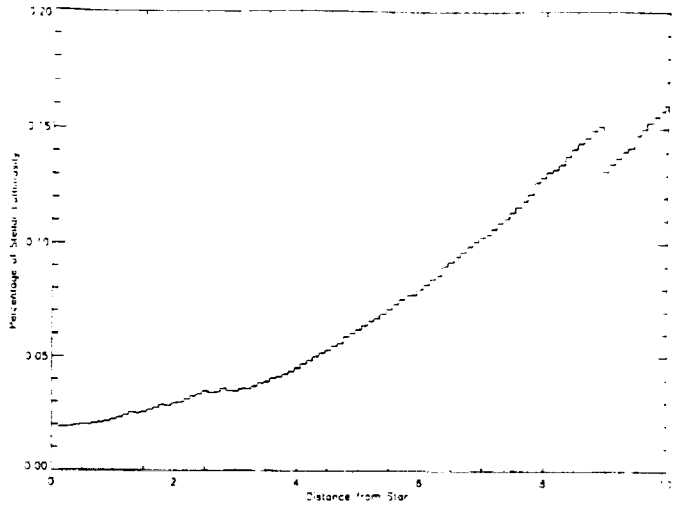

FIG. 12.—The emission within a series of circles around the central star is plotted as function of the radius of the circle as a percentage of the total stellar luminosity. Even within 10 pc of the star, much less than 1% of the stellar flux is emitted within the *IRAS* bands.

4. SUMMARY

We have detected 123 clouds (Table 2) around 106 of a sample of 745 stars for a number fraction of 0.14 ± 0.05. These clouds are similar in properties (Table 4) to those clouds which make up the WIM of McKee & Ostriker (1977) and may form a subsample of that group. If we ignore selection effects, important as they may be in this work, we obtain an average intercloud separation of 46 pc and a volume filling factor of 0.006, much lower than the 0.23 in the McKee-Ostriker theory. There is very little material around the stars except for the clouds, and we place upper limits of abut 0.05 cm^{-3} on the average gas density, which is weighted heavily by the emission near the brightest stars in our survey. We note that this implies that the density of any smooth component of the ISM must be less than this value and that most of the matter must be in the form of discrete clouds, either the diffuse clouds we sample or cold, dark clouds. As a corollary, most of the stellar ionizing flux escapes the neighborhood of the stars into the ISM as a whole.

The latitude dependence of the clouds is fitted reasonably well by a cosecant distribution, except at high galactic latitudes. If one restricts the sample to only the most luminous stars, the falloff with increasing latitude is much less, perhaps reflecting a more uniform distribution of dust once out of the Galactic disk. If we divide our sample into two groups based on luminosity, we find exponential scale heights of 140 and 540 pc for the less luminous and more luminous stars, respectively, again perhaps reflecting differing distributions of dust. We have also found significant numbers of clouds at quite large distances from the Galactic plane.

If our tentative identification of these clouds with the WIM is correct, studying their distribution will yield important clues to the nature of the ISM. We plan to perform Monte Carlo simulations to further understand our observed distribution and the selection effects inherent in our method. We are also studying the individual clouds to study the effects of stellar processing on the dust grains. With the wide range in the radiation fields in our survey, both in intensity and in hardness, we hope to be able to pin down the variations in the properties of the dust as a function of radiation processing and thereby place strong constraints on the physical nature of the dust.

We are grateful to M. Werner, C. Allen, J. Wofford, R. Kimble, C. Mullis, and M. Earl for their contributions to this project. We thank F. Verter and the referee, A. N. Witt, for pertinent comments on the manuscript. Some of this work was done while J. M. was a NRC/NAS Resident Research Associate at NASA/GSFC and this work was supported through NAG-51282. H. J. W. is grateful to the Johns Hopkins University for a visiting fellowship and her work, while at NASA/Ames Research Center, was funded through the SETI Institute under cooperative agreement NCC 2-407. The Bright Star Catalog, SKYMAP, and the *IRAS* Skyflux plates were provided by the National Space Science Data Center and several IDL programs were obtained from the IDL Users Astronomy Library at NASA/GSFC.

REFERENCES

Bohlin, R. C., Savage, B. D., & Drake, J. F. 1978, ApJ, 224, 132
Boulanger, F., Falgarone, E., Puget, J. L., & Helou, G. 1990, ApJ, 364, 136
Boulanger, F., & Perault, M. 1988, ApJ, 330, 964.
Bruhweiler, F. C., & Vidal-Madjar, A. 1987, in Exploring the Universe with the *IUE* Satellite, ed. Y. Kondo (Dordrecht: Reidel), 467
Burstein, D., & Heiles, C. 1978, ApJ, 225, 40
Burton, W. B., Walker, H. J., Deul, E. R., & Jorgenleen, A. W. W. 1986, in Light on Dark Matter, ed. F. P. Israel (Dordrecht: Reidel), 357
de Vries, C. P. 1985, A&A, 150, L15
Desert, F. X., Boulanger, F., & Puget, J. L. 1990, A&A, 237, 214
Draine, B. T., & Lee, H. M. 1984, ApJ, 285, 89
Feitzinger, J. V., & Stuwe, J. A. 1986, ApJ, 305, 534

Franco, J., Ferrini, F., Ferrara, A., & Barsella, B. 1991, ApJ, 366, 443
Gottlieb, D. M. 1978, ApJS, 38, 287
Heiles, C. 1975, A&AS, 20, 37
——— 1976, ApJ, 204, 379
Hoffleit, D. 1982, The Bright Star Catalog (4th rev. ed.; New Haven: Yale Univ. Obs.)
Hurwitz, M., Bowyer, S., & Martin, C. 1991, ApJ, 372, 167
IRAS Explanatory Supplement. 1986, ed. C. A. Beichman, G. Neugebauer, H. J. Habing, P. E. Clegg, & T. Chester (Washington: GPO)
Knude, J. 1979, A&A, 77, 198
———. 1981, A&A, 98, 74
Kulkarni, S. R., & Heiles, C. 1987, in Interstellar Processes, ed. D. J. Hollenbach & H. A. Thronson, Jr. (Dordrecht: Reidel), 87
Kurucz, R. 1979, ApJS, 40, 1
Leisawitz, D., & Hauser, M. G. 1988, ApJ, 332, 954
Lockman, F. J., Hobbs, L. M., & Shull, J. M. 1986, ApJ, 301, 380
Low, F. J., et al. 1984, ApJ, 278, L19
McKee, C. F., & Ostriker, J. P. 1977, ApJ, 218, 148
Murthy, J., Henry, R. C., & Holberg, J. B. 1991, ApJ, 383, 198
Reynolds, R. J. 1990a, IAU Symp. 139, The Galactic and Extragalactic Background Radiation, ed. S. Bowyer & C. Leinert (Dordrecht: Kluwer), 157
Reynolds, R. J. 1990b, ApJ, 345, 811
Sanders, D. B., Scoville, N. Z., & Solomon, P. M. 1985, ApJ, 289, 373
Van Buren, D. 1989, ApJ, 338, 147
Van Buren, D., & McCray, R. 1988, ApJ, 329, L93
Zombeck, M. V. 1982, Handbook of Space Astronomy and Astrophysics (Cambridge: Cambridge Univ. Press)

NOB

THE DISTRIBUTION OF DUST CLOUDS IN THE INTERSTELLAR MEDIUM

ANDREW R. DRING,[1] JAYANT MURTHY,[1] R. C. HENRY,[1] AND H. J. WALKER[2]

[1]Department of Physics and Astronomy, The Johns Hopkins University, Baltimore, MD 21218

[2]DRAL, Rutherford Appleton Labs, Chilton, Didcot, Oxon, United Kingdom.

Received 1994

ABSTRACT

Murthy, Walker, & Henry (1992) examined 745 O, B, F and G stars on the IRAS Skyflux plates, and 123 clouds near 106 stars were found. We have performed further modeling to understand the statistical cloud distribution in the interstellar medium. We were unable to find a single component fit to the entire data set, however, if we ignored the luminous O stars, a model fit with the parameters: filling factor = 0.166, scale height z = 131, a radius power-law exponent α = -2.39 and a density power-law exponent β = -1.0 was found where the filling factor includes material in the density ranges 0.001-100 H cm^{-3}. There was much less dust in the vicinity of the O stars. We find a filling factor of ($0.02\ ^{+\,0.01}_{-\,0.005}$) for dust of density greater than ~10.0 H cm^{-3} to which we are complete.

Subject Headings: interstellar: matter - nebulae: reflection

1. INTRODUCTION

The main components of the emission detected by the Infrared Astronomical Satellite (IRAS) in the 60 and 100 μm bands are due to zodiacal light and cool cirrus clouds heated by the interstellar radiation field (ISRF) . Some of these clouds may lie near enough to a luminous star that dust heating due to the star is sufficient to let the discrete cloud be distinguished from the cooler cirrus clouds. By surveying luminous stars at known distances from the sun, a rough three dimensional map of the dust distribution can be obtained. Furthermore, if we treat the stars as a random sampling of the interstellar medium (ISM), we can compare our observations of dust-heated clouds to model cloud distributions in the ISM. This is a powerful probe of the statistical properties of the ISM, including its filling factor and the degree to which matter is distributed randomly.

The first attempt at such observations was performed by Van Buren (1989), who looked at a limited region of the sky near the Galactic plane and found a volume filling factor of 0.2 ± 0.1. More recent attempts have been made by Murthy, Walker & Henry (1992), who looked at a sample of 745 luminous stars from the *Bright Star Catalogue* (Hoffleit 1982), excluding regions of the galactic disk, and by Gaustad & Van Buren (1993) who looked at all 1808 O and B stars from the *Bright Star Catalogue*. They found filling factors of 0.006 ± 0.002 and 0.146 ± 0.024 respectively. Murthy et al. set an upper limit on the pervading gas density of 0.05 cm^{-3} and reported two dust scale heights of 540 pc and 140 pc for dust associated with more luminous and less luminous stars respectively. Gaustad & Van Buren did not attempt to set limits on the pervading gas density or measure the dust scale height but they did suggest that the dust distribution was trough-like near the sun and correlated with Gould's belt (Stothers & Frogel 1974).

The present work utilizes the sample of Murthy et al. and tries to understand some of the many selection effects by using more detailed cloud distribution models and Monte

Carlo simulations. We find that there are significant differences in the amount of dust near O and B star populations, and we were only able to find an acceptable model for the dust associated with the B stars. This model, excluding O stars which have very little dust nearby, gives a better estimate of the filling factor for gas with equivalent densities above ~10.0 cm^{-3} to which our survey is complete. We find a revised filling factor of $(0.02\ ^{+0.01}_{-0.005})$, which is still lower than Gaustad & Van Buren but is applicable only to dust in the higher density range. The model also shows that the best fit to the scale height of the dust is 130 pc although there are several clouds at very high z which are hard to explain with such a small scale height.

2. DATA SET

The survey by Murthy et al. used *IRAS* Skyflux plates in the vicinity of 745 stars selected primarily from the *Bright Star Catalog* (see Murthy et al. for details). They excluded regions within 10 degrees of the galactic plane and also excluded several regions of known molecular cloud concentrations, such as Orion and Taurus. The spectral type, apparent magnitude, and observed B-V for each star were obtained from the *Bright Star Catalog*, while the absolute magnitude, temperature, and intrinsic B-V were read from tables in Zombeck (1982), and the E(B-V), spectroscopic distance, and luminosity of the star were calculated from the other quantities.

The Skyflux plates use only one third of the total IRAS data and have not been processed to remove either zodiacal light or instrumental artifacts and are less sensitive then the *Infrared Sky Survey Atlas* (ISSA), which are essentially Bigmaps. To quantify the difference in the data sets, we examined a limited set of 179 stars for which we had both Skyflux and ISSA data. We used two sets of search criteria, similar but not identical to the methods used by Murthy et al. and Gaustad & Van Buren. Both techniques were performed automatically by a computer program and applied equally to

the ISSA plates and the Skyflux plates. Using method one we found 26 clouds on the ISSA plates, 7 of which were also on the Skyflux plates. Using method two we found 34 clouds on the ISSA plates, 8 of which were on the Skyflux plates. There were no clouds found on the Skyflux plates that were absent on the ISSA plates. Thus when the same method is applied to the two different data sets, we find roughly a factor of four times more clouds on the ISSA plates than the Skyflux plates. This implies that Gaustad & Van Buren should be detecting fainter clouds than Murthy et al.

Figure 1 shows histograms for the flux, surface brightness, density and size for both the Murthy et al. data and the data from Gaustad & Van Buren. The flux, density and radius were taken from columns 10, 15 and 13, respectively, in Table 2 of Gaustad & Van Buren and the surface brightness was calculated by dividing column 10 by the square of column 13 multiplied by π. The clouds of Gaustad & Van Buren are larger and have lower surface brightness and densities. (There was an error in the Murthy et al. paper which mistakenly labelled column 7 as the radius when in fact it was the diameter. As a result the individual cloud densities in column 9 of the Murthy et al. paper are too low by a factor of eight and their filling factor is too high by the same factor. All other quantities remain the same.) It is apparent that the better data used by Gaustad & Van Buren enable them to see larger, lower surface brightness objects, and therefore lower density material. As will be shown later this implies that the filling factor for Gaustad & Van Buren should be higher than for the Paper I clouds.

3. MODELLING

We would like to understand how dust is distributed in the galaxy by comparing the predictions of various dust distribution models with observations. In order to make the comparison we need to understand how dust in the vicinity of a hot star will appear to IRAS. Thus before discussing the dust distribution models, we must construct a detailed

model for dust heating and emission in clouds near stars. Consider a volume element $dV = R^2\, d\Omega\, dr$ a distance R away from the illuminating star. The energy absorbed by dust in this volume at a given wavelength is:

$$\Delta E_\lambda = \frac{d\Omega}{4\pi} L_\lambda \left(\exp(-\tau_\lambda) - \exp(-\tau_\lambda - d\tau_\lambda) \right) (1-a_\lambda) \tag{1}$$

where L_λ is the luminosity of the star at a given wavelength, a_λ is the albedo at that wavelength, τ_λ is the optical depth from the star to the volume element and $d\tau_\lambda$ is the optical depth of the volume element. In all the clouds considered, $\tau_\lambda << 1$, so we assume optically thin nebulae and get:

$$\Delta E_\lambda = \frac{d\Omega}{4\pi} L_\lambda d\tau_\lambda (1-a_\lambda) \tag{2}$$

Using a gas to dust ratio of $N_H / E(B-V) = 5.8 \times 10^{21}$ atoms cm^{-2} mag^{-1} (Bohlin, Savage & Drake 1978), which is used throughout this work, we have:

$$d\tau_\lambda = \frac{1}{1.086} \frac{A_\lambda}{A_V} \left(\frac{N_H R_V}{5.8 \times 10^{21}} \right) = 4.9 \times 10^{-4} \frac{A_\lambda}{A_V} n_H R_V dr \tag{3}$$

where A_λ/A_v is the extinction law of Cardelli, Clayton & Mathis (1989) with R_V=3.1, n_H is the gas density in H cm^{-3} and dr is measured in parsecs. Combining to get the energy density of absorbed radiation we have

$$dE/dV = 1.33 \times 10^{-60}\, n_H\, L_{eff}\, R_{pc}^{-2} \text{ erg } s^{-1}\, cm^{-3} \tag{4}$$

where

$$L_{eff} \equiv \int L_\lambda \frac{A_\lambda}{A_V} (1-a_\lambda) d\lambda \tag{5}$$

Thus we see that what is important is not the bolometric luminosity but an effective luminosity which takes account of the optical properties of the dust. Table 1 compares the effective luminosity with the bolometric luminosity for several spectral types. The effective luminosities in this work were calculated using Kurucz (1979) model

atmospheres for the stars and grain albedos from Draine & Lee (1984). Assuming that all the energy absorbed is reradiated isotropically in the infrared, the emissivity is just $dE/4\pi dV$. Using dust properties from Draine & Lee, we equate grain heating to cooling and integrate over grain sizes to obtain the temperature:

$$T = 1.54 \times 10^5 \, (dE/dV n_H)^{1/6} = 42.0 \, Leff_{38}^{1/6} \, R_{pc}^{-1/3} \; K \qquad (6)$$

This is essentially the same as equation (1) of Gaustad & Van Buren except that it correctly accounts for the hardness of the radiation by using the effective luminosity. Table 1 shows the difference between equation (6) and that of Gaustad & Van Buren for R=1 pc, which is largest for early B stars. Finally, with an estimate of the geometry, one can generate an image in any desired IRAS band by convolving the dust emission profile with the instrument response function.

To understand how dust is distributed in the galaxy, we compute the number of nebulae we expect to see for each star for a given cloud distribution model and compare with our observations. To compute the expected number of nebula for each star we consider a large volume of the galaxy, s^3, as shown in Figure 2. If we use spherical clouds of uniform density and distribute them randomly throughout the volume then we can compute the probability for each cloud that it will be close enough to the star to be observed. For a star with a given L_{eff} and a cloud with a given radius and density we can compute the maximum distance (d_{max}) out to which the cloud may be seen given the spatial resolution and sensitivity of IRAS. The probability that the cloud is observed is just $4\pi/3(d_{max}/s)^3$. We can then integrate over all clouds to compute the expected number of nebula for each star, with a lower size cutoff for unresolved clouds. The predicted number of observed nebulae for any subgroup of stars can be directly compared with the observations using a χ^2 analysis. The cloud distribution model uses a power-law distribution for the cloud radius with exponent α, a power-law distribution for the dust density in the cloud with exponent β, and a single component exponential scale

height z. The volume filling factor is just the total volume of clouds divided by the total volume of our sample space.

4. RESULTS

Since the radiation fields differ dramatically for different spectral types, it is important to separate the sample of Murthy et al. into subgroups based on their effective luminosity. Figure 3 shows a histogram of the sample binned according to L_{eff}, with representative spectral types for each bin. Figure 4 shows a histogram of the number of nebulae found in each bin divided by the number of stars with an estimate of the uncertainty, assumed to be the square root of N, shown by the errorbars. We allowed the volume filling factor, scale height and power law exponents for size and density of the nebulae to vary freely and attempted to find the parameter values which could best reproduce our observations. The best fit to the data using all bins is shown as plus signs in Figure 4 and uses the parameters: filling factor=0.172, z=133, the radius power-law exponent α = -1.23 and the density power-law exponent β = -0.25 which produced a reduced $\chi_5^2 = 5.1$.

An important assumption of this model is that the clouds are distributed randomly with respect to the stars, and the poor fit implies this assumption is incorrect. In particular it is apparent that fewer dust clouds are predicted near B stars than are observed. We then attempted to fit just the B stars which correspond to the first six bins in Figure 4. The best fit model gave the parameters: filling factor = 0.166, z = 131, α = -2.39 and β = -1.0 with a resulting reduced $\chi_2^2 = 3.85$. This model is shown in Figure 4 as diamonds. Although still not particularly good, the B star fit is significantly better than the fit for all stars. Finally the B star model predicts too many clouds for the O stars and gives essentially the same filling factor and scale height as the fit for all stars.

The filling factor of 0.16 for the B stars is slightly lower than the filling factor of 0.25 of McKee & Ostriker (1977) for the warm ionized medium. The power-law index for the size distribution $\alpha = -2.39$ is inconsistent with the value $\alpha = -4.0$ in McKee & Ostriker but it agrees well with the value $\alpha = -2.6$ of Knude (1981) and with the value of $\alpha = -2.3$ of Sanders, Scoville & Solomon (1985) although the latter looked at dense CO clouds which may not be comparable to the clouds in the Murthy et al. survey. Our scale heights are consistent with estimate of Nandy et al. (1978) of $z = 110$ pc for the agent of extinction at 2200 A. There are few published values for the power-law index of the density distribution but an analysis of Figure 5 in Knude (1979) gives $\beta = -0.5$, which is marginally consistent with our value of $\beta = -1.0$.

The failure of our models to predict the number of clouds near O stars indicates that the clouds are not distributed randomly; there are far fewer clouds near O stars than would be predicted. There are several reasons for believing that the dust is not distributed randomly. One might expect that early type stars would tend to be younger and still associated with their pre-natal clouds, increasing the probability of finding clouds near those stars, however this effect would not be important for the Murthy et al clouds since they exclude regions of star formation. Conversely, early type stars have much more intense radiation fields and are more likely to strongly affect their nearby environment by removing, destroying or changing the optical properties of dust. Also since we have excluded those regions where O stars are usually found, this suggests that the O stars in our sample are atypical in some way. This may provide an explanation for the dearth of clouds near O stars found in this survey.

The method used to calculate the filling factor in Murthy et al. is particularly sensitive to the estimate of the total volume probed. This volume was estimated by determining the point at which the ISRF became equal to the radiation field of the star in question. A second way to estimate this volume is to use equation (5) for the temperature as a function of distance from the star. Since the temperature depends on the

distance to the 1/3 power, the total volume probed goes as T^6, but we can make a more accurate estimate of the average interstellar temperature, or more appropriately the effective limiting temperature for observing a cloud. Figure 5 shows a histogram of the number of clouds as a function of their 60/100 μm ratio for the Murthy et al. clouds. Although model dependant, we have calculated temperatures using an emissivity proportional to ν^2 and plotted them across the top. The distribution falls off rapidly below 30K and the coldest cloud observed is 24.3 ± 1.5 K where the uncertainty is found by using the standard deviation for the cloud in the 60 μm band. Using the most conservative limit of 24.3 ± 1.5 K for the minimum temperature needed to observe a cloud, the total volume probed is $6.4 \pm 2.4 \times 10^5$ pc^3 for all stars and $5.5 \pm 2.0 \times 10^4$ pc^3 for just the B stars. Using a cloud volume of 5×10^3 pc^3 for all stars and a cloud volume of 1.1×10^3 pc^3 for B stars we obtain a filling factors of $(0.008\ ^{+0.004}_{-0.002})$ and $(0.02\ ^{+0.01}_{-0.005})$, respectively, for dust of equivalent density greater than ~10.0 H cm^{-3}. The filling factor for all stars is more than a factor of two lower because the O stars constitute over 90% of the total volume probed, independent of the method used to determine the total volume, and there are few clouds associated with the O stars. To compare this estimate with our model we need to remember that the filling factor of 0.166 in our model is for dust with densities in the range 0.001-100 H cm^{-3}. The fraction of dust greater than ~10.0 H cm^{-3} for our power-law of $\beta = -1.0$ is 0.2 yielding a filling factor of 0.032 for our model in the appropriate density range.

While it is convenient to quote filling factors as a single number, it is important to remember that they are a function of density. Figure 6 shows the upper limit of the filling factor as a function of density that was calculated on a pixel by pixel basis. The upper limit was calculated by assuming that all the emission in a given pixel was thermal emission from hot dust near the star. The space density was obtained by dividing the intersection of our line of sight with the sphere of influence of the star into the column density. As seen in the figure, the filling factor of dust of density greater than

~0.5 H cm^{-3} lies below 0.191 and for dust of density greater than ~10.0 H cm^{-3} lies below 0.085 for the region of space near the stars in our survey. It should be remembered that this limit includes all the dust after smooth background subtraction, and that the true filling factor for this density range will be lower.

5. COMPARISON WITH GAUSTAD AND VAN BUREN

Our improved value for the filling factor of $(0.02\ ^{+0.01}_{-0.005})$ is a factor of three closer to Gaustad & Van Buren's value of 0.142 ± 0.024 but is still lower by almost a factor of ten. The difference is probably not a result of the inclusion of regions where there are known dust clouds, since Gaustad & Van Buren's estimate of the filling factor where the samples overlap is 0.154. One explanation proposed by Gaustad & Van Buren is that their data set is more sensitive than the Murthy et al. data set. As was shown in Figure 1, the clouds of Gaustad & Van Buren have lower surface brightness than the Murthy et al. clouds and a lower density by more than a factor of ten. We have also seen in Figure 6 that the filling factor is a strong function of density and therefore the filling factors quoted by Gaustad & Van Buren and Murthy et al. are consistent given the density of material they are sampling.

An alternate method of computing the filling factor is that of Gaustad & Van Buren, which is to take the fraction of stars with dust clouds centered on the star. This valid if the stars can be treated as pointlike probes, however in the Murthy et al. data almost half of the listed clouds do not exhibit a spherically symmetric morphology and are not centered on the star. Using this method we obtain a filling factor of 0.07, which is still a factor of two below that of Gaustad & Van Buren, but this is consistent with the fact that they are observing lower density material.

6. CONCLUSION

The technique of searching near luminous stars for heated dust is a powerful probe of the interstellar medium. The value of the filling factor quoted in Murthy et al. was found to be too low, mostly due to the inclusion if O stars which had surprisingly little dust nearby. Using the coldest observed cloud to determine the total volume probed we obtain a value of ($0.008 \,^{+0.004}_{-0.002}$) and ($0.02 \,^{+0.01}_{-0.005}$) for all stars and B stars respectively. This filling factor is still lower than the value of 0.142 ± 0.024 quoted by Gaustad & Van Buren, but this is mostly due to the fact that Gaustad and Van Buren are observing lower density material and the filling factors are consistent for the densities observed.

We could not fit our observations with a single component model and were forced to fit the B stars only which resulted in a filling factor of 0.166 for dust in the density range 0.001-100 H cm^{-3} in the vicinity of our program stars. There was a significant paucity of dust near the O stars which suggests that this may be a special environment. The small amount of dust near O stars means that a significant amount of ultraviolet radiation must escape from the O stars and become part of the ISRF. Our models also gave estimates of 130 pc, -2.5, and -1.0 for the scale height of the dust, the spectral index of the cloud sizes, and the spectral index of the cloud densities respectively in fair agreement with other published values.

TABLE 1

COMPARISON OF LUMINOSITY AND EFFECTIVE LUMINOSITY

Spectral Type	L (L_{sun})	L_{eff} (L_{sun})	T (R=1pc) (K)	T_{eff} (R=1pc) (K)
(1)	(2)	(3)	(4)	(5)
B9V	95	79	15.9	15.4
B5V	830	970	22.8	23.3
B2V	5700	12900	31.4	36.0
O8V	170000	189000	55.3	56.3

Notes: Column (2) is the bolometric luminosity for the star and column (3) is the computed effective luminosity for the same star. The effective luminosity is essentially normalizing the luminosity to given temperature and is thus larger than the bolometric luminosity for hotter stars and less than the bolometric luminosity for cooler stars. Columns (4) and (5) are the dust grain temperatures computed from columns (2) and (3) respectively.

REFERENCES

Bohlin, R.C., Savage, B. D., & Drake, J. F. 1978, ApJ, 224, 132.

Draine, B. T., & Lee, H. M. 1984, ApJ, 285, 89.

Cardelli, J. A., Clayton, G. C., & Mathis, J. S. 1989, ApJ, 345, 245.

Gaustad, J. E., & Van Buren, D. 1993, PASP, 105, 1127.

Hoffleit, D. 1982, *The Bright Star Catalog, 4th Revised Edition*, Yale Univ. Obs. (New Haven)

Knude, J. 1979, A&A Suppl, 38, 407.

Knude, J. 1981, A&A, 98, 74.

Kurucz, R. 1979, ApJS, 40, 1.

McKee, C. F., and Ostriker, J. P. 1977, ApJ, 383, 198.

Murthy, J., Walker, H. J., & Henry, R. C. 1992, ApJ, 401, 574

Nandy, K., Thompson, G. I., Carnochan, D. J. & Wilson, R. 1978, MNRAS, 184, 733.

Sanders, D. B., Scoville, N. Z., & Solomon, P. M. 1985, ApJ, 289, 373.

Stothers, R., & Frogel, J. A. 1974, AJ, 79, 456.

Van Buren, D. 1989, ApJ, 338, 147.

Zombeck, M. V. 1982, *Handbook of Space Astronomy and Astrophysics*, Cambridge University Press (Cambridge)

FIGURE CAPTIONS

FIG. 1. - Histogram plots for the flux, surface brightness, density and size distributions in units of Jy, MJy sr^{-1}, H cm^{-3}, and arcmin respectively. The dotted lines represent the data from Gaustad & Van Buren and the solid lines represent the Murthy et al. data. The flux and surface brightness plots are for the 60 μm band. Gaustad & Van Buren are clearly observing larger, less dense, and lower surface brightness clouds then Murthy et al. which implies they should observe a higher filling factor.

FIG. 2. - Method used to compute the expected number of clouds for each star. When the effective luminosity, cloud radius, density, resolution and sensitivity of IRAS are all given, it is straightforward, given the dust emission model in the text, to compute the maximum distance out to which the cloud can be seen. The probability that the cloud will be detected is $4\pi/3(dmax/s)^3$ and integrating over all clouds gives the expected number of observed clouds for each star.

FIG. 3. - A histogram of the number of stars as a function of their effective luminosity for the Murthy et al. sample with a bin size of 0.5 erg s^{-1} mag^{-1}. For reference a typical spectral type is printed over each bin.

FIG. 4. - A histogram of the number of nebulae divided by the number of stars as a function of the effective luminosity of the associated stars with a bin size of 0.5 erg s^{-1} mag^{-1}. The plus signs represent the lowest reduced chi-square model for all the stars with the parameters: filling factor= 0.172, z=133 pc, α= -1.23 and β= -0.25 and a reduced reduced χ_5^2 = 5.1. The diamonds are the best fit to the B stars with only the first six data points shown and use the parameters: filling factor= 0.166, z=131 pc, α= -2.39 and β= -1.0 and a resulting reduced χ_2^2 = 3.85.

FIG 5. - A histogram of the number of clouds with a given 60/100 um ratio. The top of the plot gives the equivalent temperature calculated using an emissivity proportional to ν^2. The coldest observed cloud, which sets a limit on the total volume probed, is 24.3K.

FIG 6. - A plot of the upper limit of the filling factor for densities greater than or equal to the abscissa. The upper limit was calculated on a pixel by pixel basis assuming all of the 60 μm emission was dust thermally heated by the star and the volume for each pixel was calculated using the intersection of our line of sight with the sphere of influence of the star. Also plotted are curves for the O and B stars alone. Notice that the filling factor is strongly dependant on the density of material observed.

Fig 1

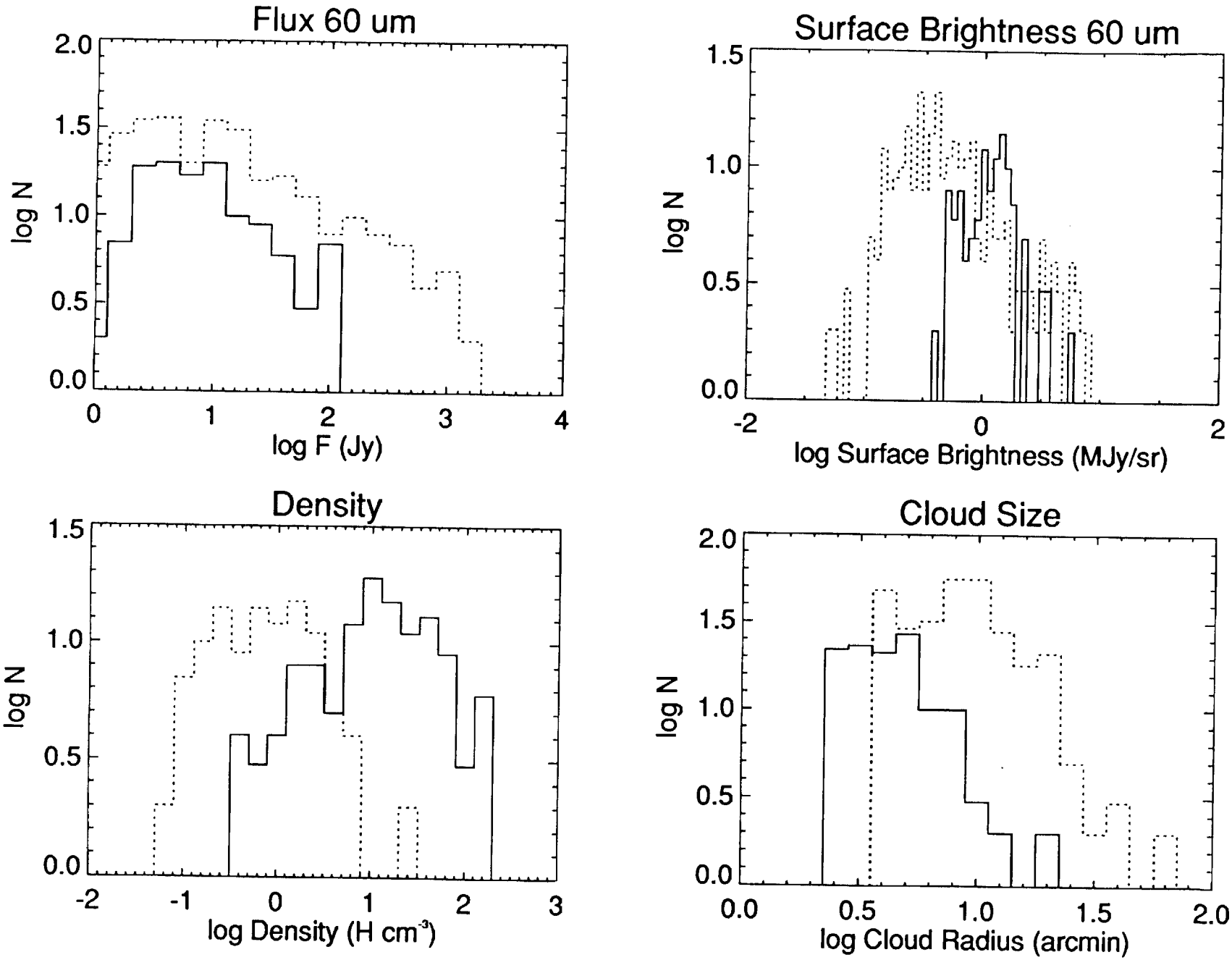
Flux 60 um
log N
log F (Jy)
Surface Brightness 60 um
log N
log Surface Brightness (MJy/sr)
Density
log N
log Density (H cm-3)
Cloud Size
log N
log Cloud Radius (arcmin)

Fig 2

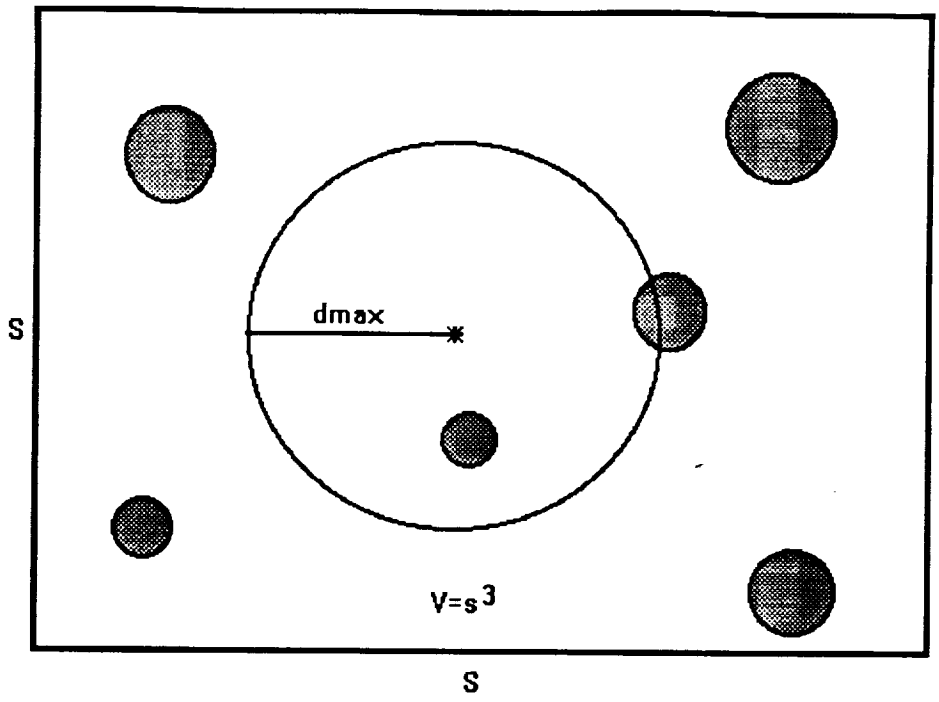

Fig 3

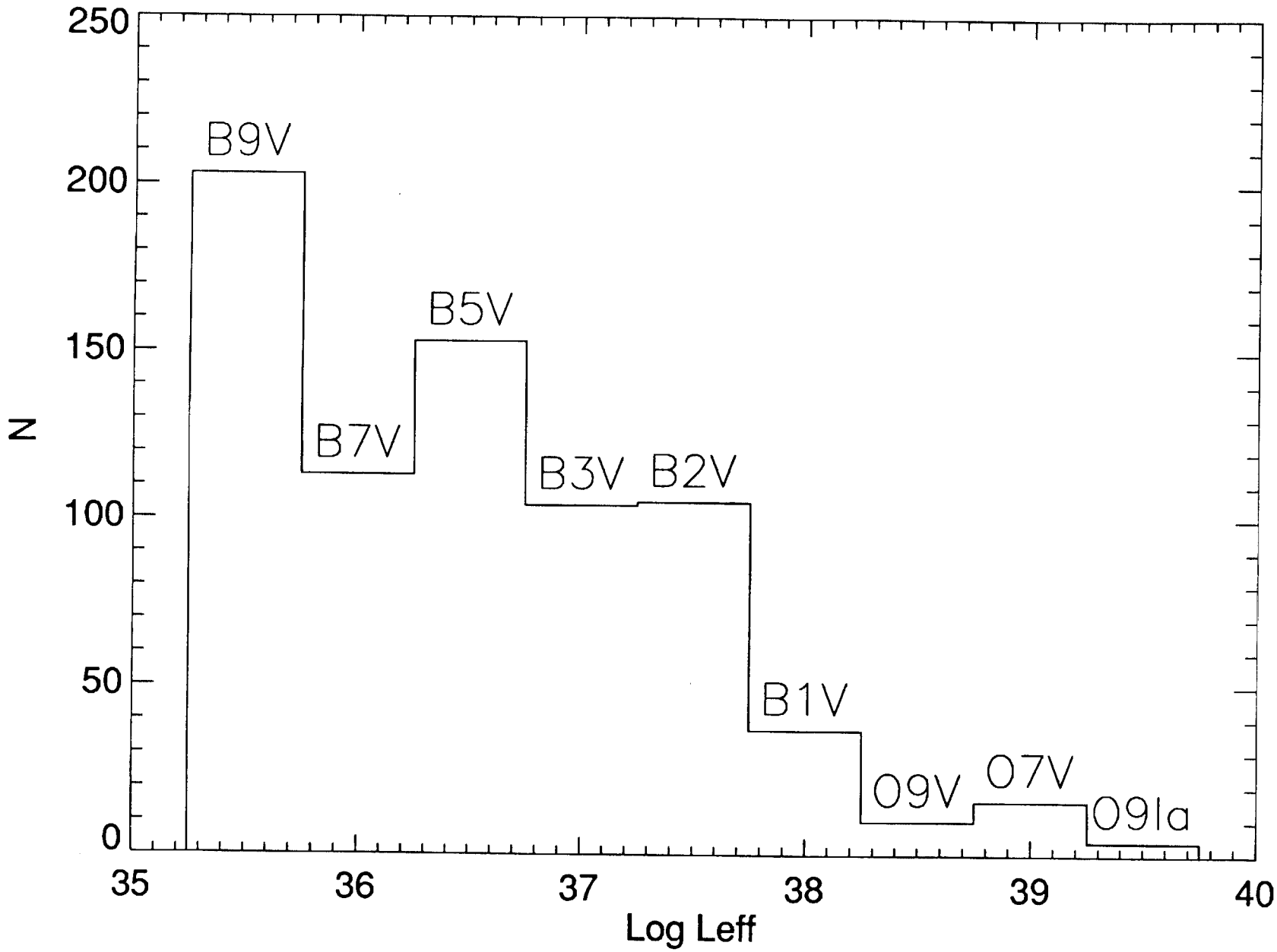
250
200
150
100
50
0
N
B9V
B7V
B5V
B3V
B2V
B1V
09V
07V
09Ia
35
36
37
38
39
40
Log Leff

Fig 4

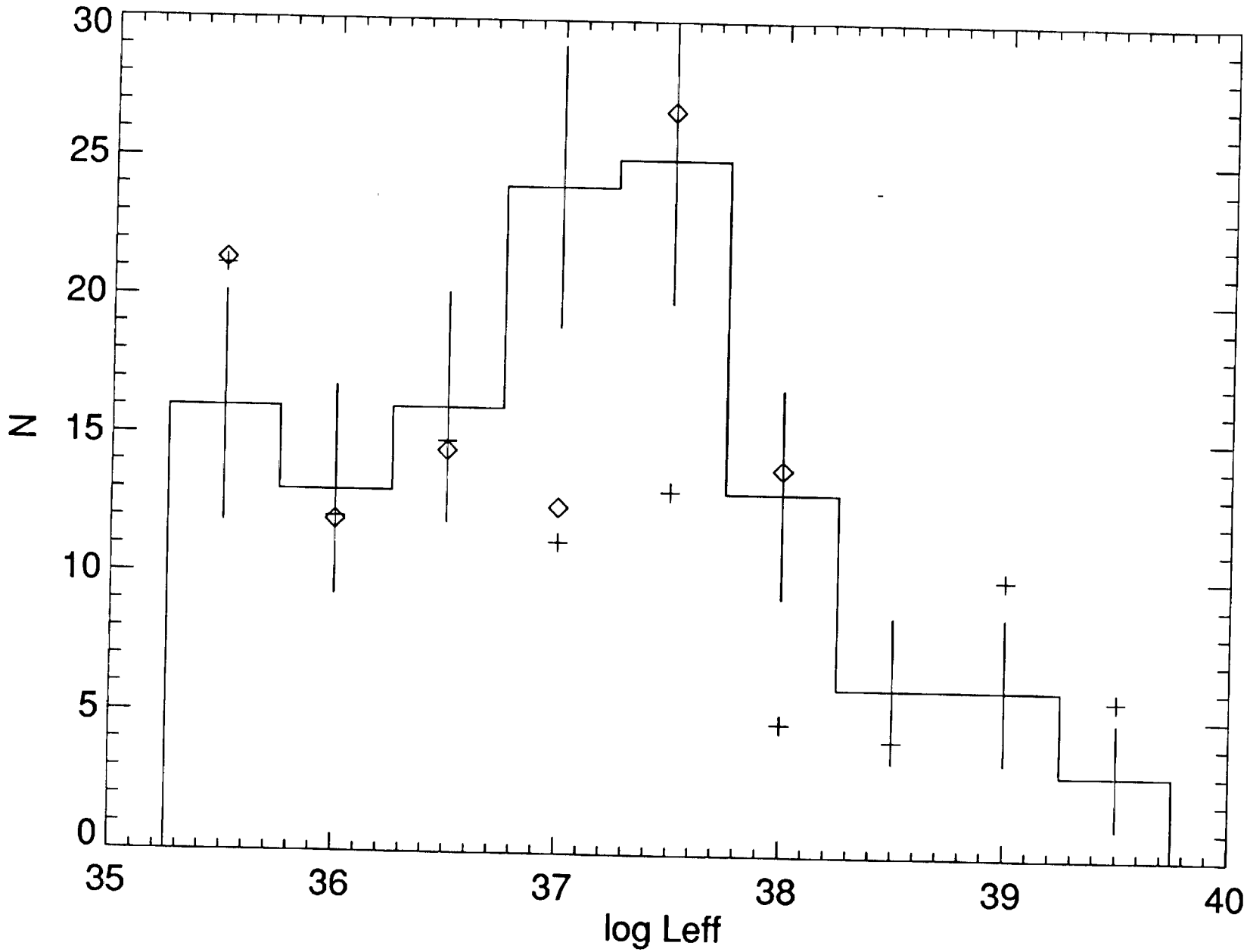

Fig 5

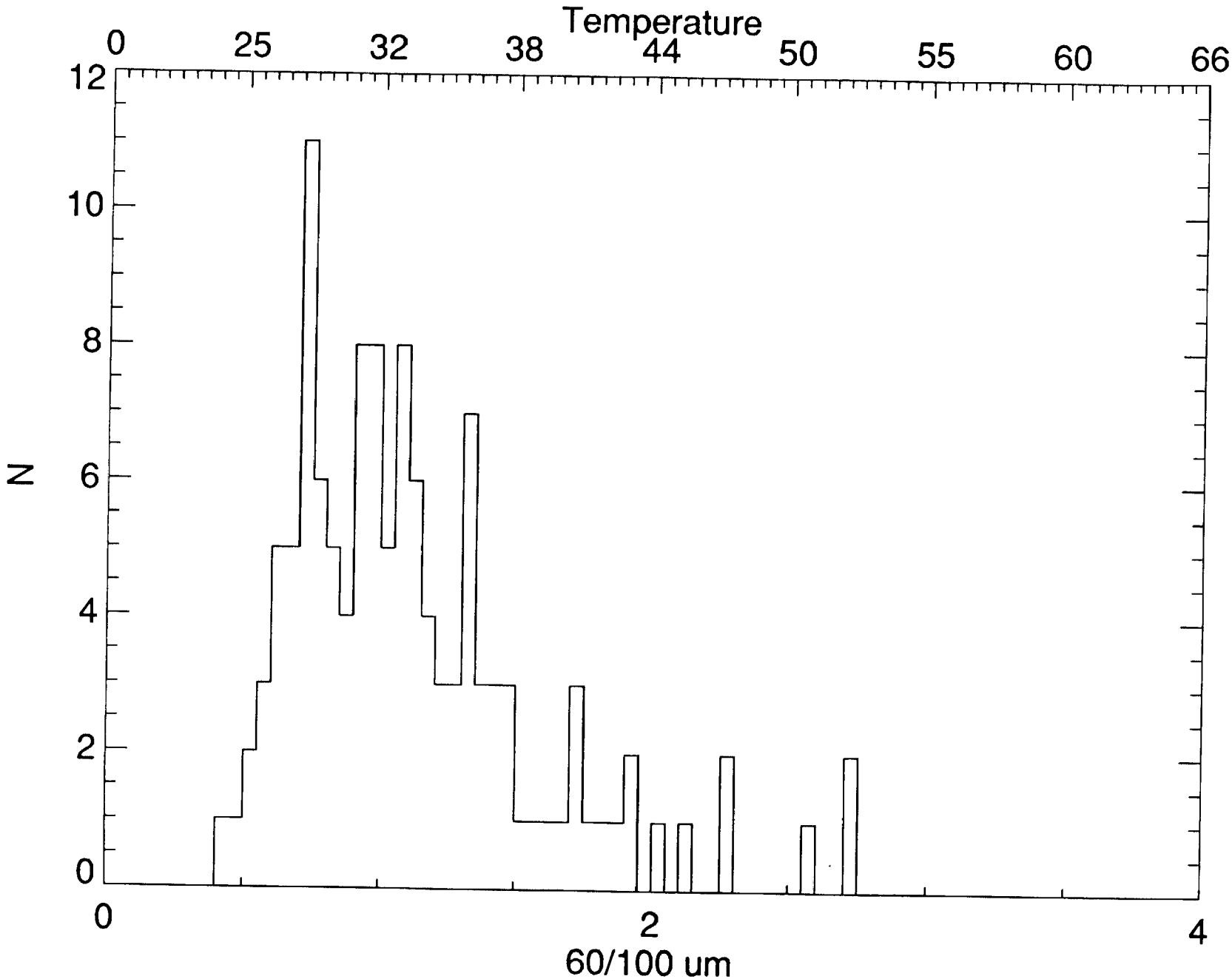

Fig 6

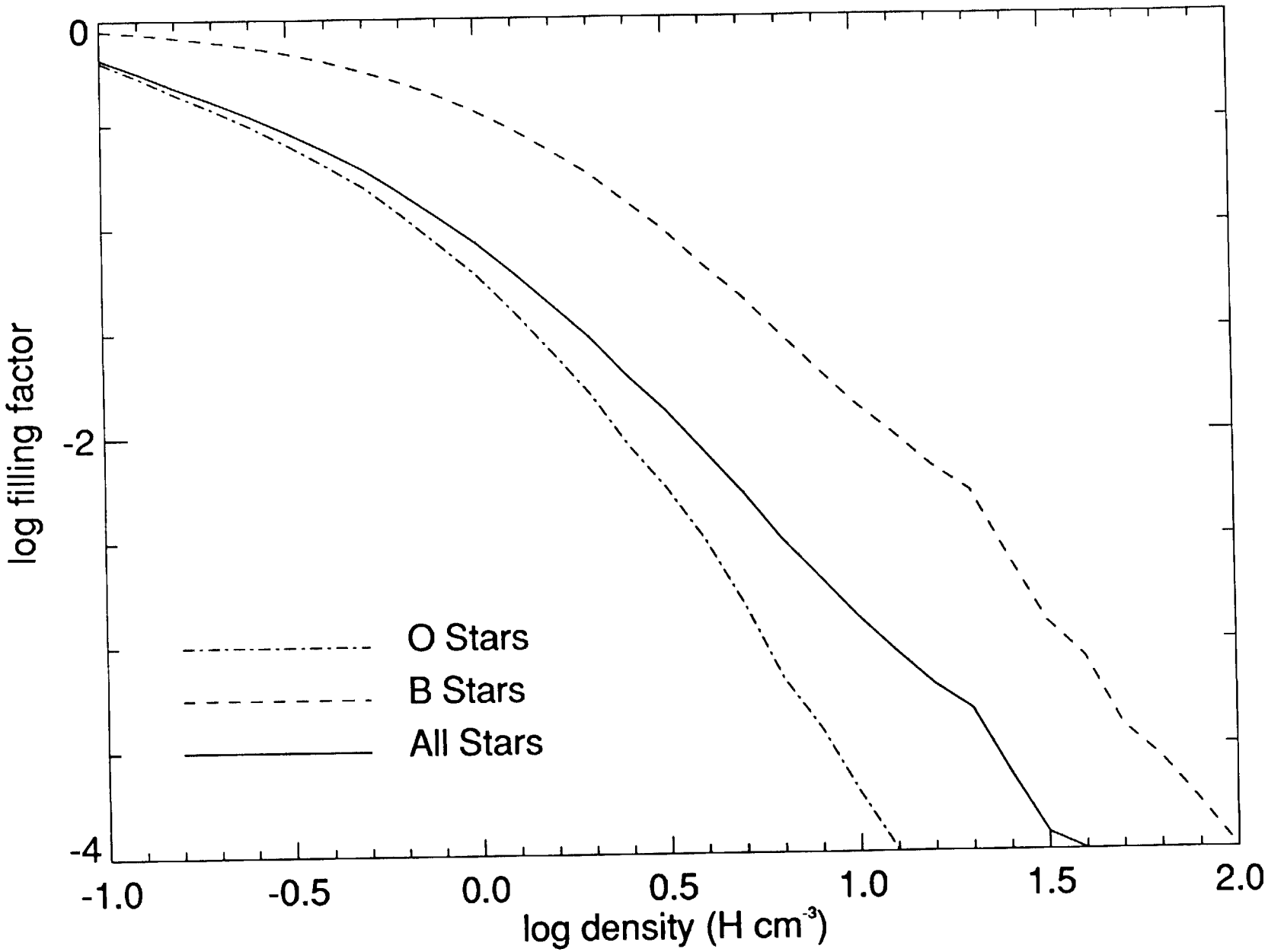
0
-2
-4
log filling factor
-1.0
-0.5
0.0
0.5
1.0
1.5
2.0
log density (H cm^{-3})
O Stars
B Stars
All Stars